PHYSICAL AND HYDROLOGIC PROPERTIES OF ROCK OUTCROP SAMPLES AT YUCCA MOUNTAIN, NEVADA

by **Lorraine E. Flint, Alan L. Flint,** U.S. Geological Survey;
Christopher A. Rautman, Sandia National Laboratories; and
Jonathan D. Istok, Oregon State University

U.S. GEOLOGICAL SURVEY

Open–File Report 95–280

Prepared in cooperation with the
NEVADA OPERATIONS OFFICE,
U.S. DEPARTMENT OF ENERGY, under
Interagency Agreement DE-AI08-92NV10874

Denver, Colorado
1996

U.S. DEPARTMENT OF THE INTERIOR

BRUCE BABBITT, Secretary

U.S. GEOLOGICAL SURVEY

Gordon P. Eaton, Director

For additional information write to:

Chief, Earth Science Investigations
Program
Yucca Mountain Project Branch
U.S. Geological Survey
Box 25046, MS 421
Denver Federal Center
Denver, Colorado 80225

Copies of this report can be purchased from:

U.S. Geological Survey
Branch of Information Services
Box 25286
Denver, Colorado 80225

CONTENTS

FIGURES

TABLES

CONVERSION FACTORS

Multiply	By	To obtain
centimeter (cm)	0.3937	inch
centimeter squared (cm^2)	0.1550	inch squared
cubic centimeter (cm^3)	0.0610	cubic inch
cubic centimeter per cubic centimeter (cm^3/cm^3)	1.0000	cubic inch per cubic inch
gram per cubic centimeter (g/cm^3)	0.0361	pound per cubic inch
kilometer (km)	0.6214	mile
megapascals (MPa)	10.0	bars
meter (m)	3.2810	feet
meter per second (m/s)	3.2810	feet per second
meter per square root of second	3.2810	feet per square root of second

Degree Celsius (°C) may be converted to degree Fahrenheit (°F) by using the following equation:

$$°F = 9/5\ (°C) + 32.$$

Degree Fahrenheit (°F) may be converted to degree Celsius (°C) by using the following equation:

$$°C = 5/9\ (°F - 32).$$

Physical and Hydrologic Properties of Rock Outcrop Samples at Yucca Mountain, Nevada

By Lorraine E. Flint, Alan L. Flint, Christopher A. Rautman, *and* Jonathan D. Istok

Abstract

A data set was developed from laboratory measurements of physical and hydrologic properties of surface outcrop samples collected from eight transects at Yucca Mountain, Nevada. Transects were located to represent the vertical and spatial variability of nonwelded and welded tuffs in major flow units. Horizontal variability was examined for several lithologic zones by conducting horizontal transects. Physical properties measured were bulk density, particle density, and porosity. Hydrologic properties were saturated hydraulic conductivity, sorptivity determined from measurements of imbibition, and moisture retention. Curves were fit to moisture-retention data using van Genuchten and Brooks and Corey equations.

Descriptive statistics of all rock properties showed major differences between nonwelded and welded units. Hydrogeologic units, based on physical and hydrologic properties, were determined to simplify flow modeling. Moisture-retention curve-fit parameters were compiled for predicting unsaturated flow. Relationships of porosity to saturated hydraulic conductivity and van Genuchten parameters were examined.

INTRODUCTION

Studies are underway at Yucca Mountain, Nevada, to characterize physical and hydrologic conditions for a potential high-level radioactive-waste repository. Site characterization requires the development of three-dimensional models describing hydrogeologic units in terms of inputs for numerical models (physical and hydrologic-flow properties). It is also important to understand the spatial distribution of these properties, vertically and horizontally, in order to estimate values at unmeasured points. Deterministic processes of volcanism caused the initial formation of the rock units, and it is useful to be able to correlate rock properties with the more qualitative descriptions of rock lithology that occur on a larger scale (Rautman and Flint, 1992).

Preliminary data were collected to develop methods and evaluate spatial relations to determine sampling frequency. In addition, a data base was developed to provide some of the parameters needed for preliminary flow-modeling exercises. Surface transects of rock outcrops facilitated rapid collection of closely spaced samples of all units exposed at and around Yucca Mountain. This report presents the data collected, descriptive statistics for various units, preliminary hydrogeologic units, and analyses of porosity compared with flow properties.

There may be skepticism associated with the use of outcrop samples, many of which have undergone some degree of weathering, to represent subsurface material properties. However, there is evidence that physical and hydrologic properties measured on outcrop samples can be predicted in boreholes (Istok and others, 1994) even when using nonwelded rocks that weather more rapidly. In addition, subsurface borehole moisture conditions have been successfully modeled using parameters developed from measurements taken on surface outcrop samples (Flint and others, 1993).

SITE DESCRIPTION AND LITHOLOGY

Yucca Mountain is 130 km northwest of Las Vegas, Nevada (fig. 1), and is composed of approximately 6 km^2 of ash-flow and ash-fall tuffs. These rocks have been tilted, faulted and eroded, and dip to the east-southeast, providing exposures of the tuffs of the Paintbrush Group and underlying tuffaceous beds of the Calico Hills Formation (fig. 2). At the north end of Yucca Mountain in Yucca Wash (fig. 1), most of the tuff of the Paintbrush Group is exposed south of Yucca Wash. The tuffs are composed of vitric to largely devitrified rhyolitic and quartz-latitic flows that range from nonwelded to densely welded rock with interbedded, nonwelded pumice and tuff. The Paintbrush Group is composed of two major thick flow units, the Tiva Canyon Tuff and the Topopah Spring Tuff. Geologic nomenclature used in this report is based on the units described by Scott and Bonk (1984). Between these members are thinly bedded and nonwelded units, as

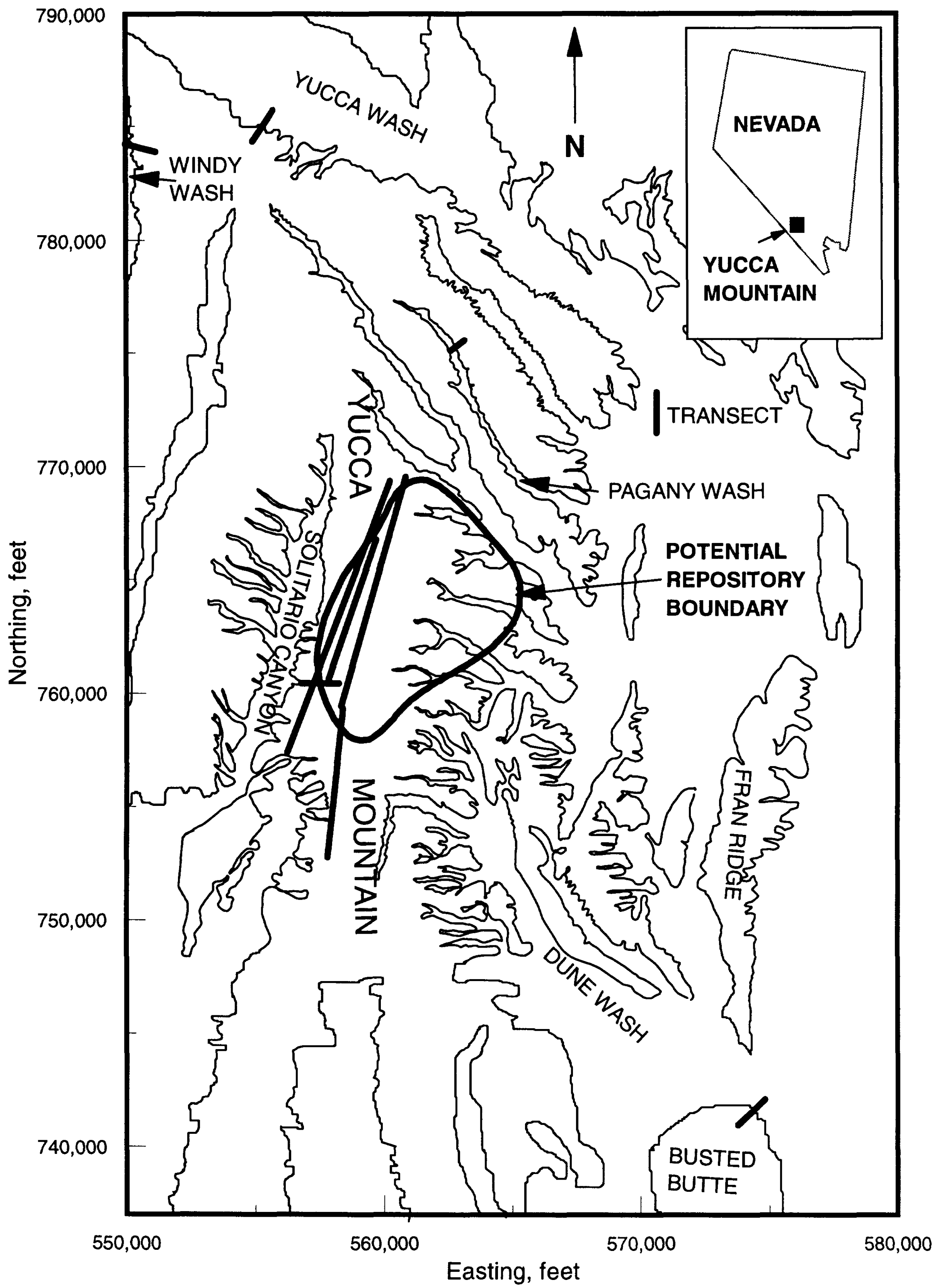

Figure 1. Study area, potential repository boundary, and location of surface outcrop-sampling transects.

Group	Geologic Unit	Informal Geologic Nomenclature	Zonation of Buesch and others(1995)	Thermal/ Mechanical Nomenclature (Ortiz and others, 1985)
Paintbrush Group	Tiva Canyon Tuff	ccr - caprock	Tpcrv	TCw
		cuc - upper cliff	Tpcm	
		cul - upper lithophysal	Tpcrl	
			Tpcpul	
		cks - clinkstone	Tpcpmn	
		cll - lower lithophysal	Tpcpll	
		ch - hackly	Tpcplnh	
		cc - columnar	Tpcplnc	
			Tpcpv3	
		ccs - shardy base	Tpcpv2	PTn
			Tpcpv1	
	Yucca Mountain Tuff			
	Pah Canyon Tuff			
	Topopah Spring Tuff	tn- upper nonwelded	Tptrv3	
			Tptrv2	
		tc - caprock	Tptrv1	TSw1
		tr - rounded	Tptrn	
		tul - upper lithophysal	Tptrl	
			Tptpul	
		tnl - nonlithophysal	Tptpmn	TSw2
		tll - lower lithophysal	Tptpll	
		tm - mottled	Tptpln	
		tv - basal vitrophyre	Tptpv3	TSw3
		nonwelded base	Tptpv2	CHn1
			Tptpv1	
Calico Hills Formation		Tht - zeolitized		
Crater Flat Group	Prow Pass Tuff	pp - prow pass		

Figure 2. Conceptual stratigraphic column showing lithostratigraphic units.

well as the Yucca Mountain and Pah Canyon Tuffs. Underlying the Topopah Spring Tuff are the tuffaceous beds of the Calico Hills Formation, which are nonwelded rocks that have been zeolitized at the north end of Yucca Mountain, yet remain vitric toward the south end of the mountain. There are no vitric rocks in the tuffaceous beds of the Calico Hills Formation exposed on or near Yucca Mountain. The Prow Pass Tuff is the most recently deposited and, therefore, the uppermost flow unit within the Crater Flat Group, which underlies the Calico Hills Formation.

The Pah Canyon and Yucca Mountain Tuffs are relatively thick to the north in Yucca Wash and contain both welded and nonwelded intervals. However, the welded units thin rapidly southward toward the proposed repository, and only thin intervals of nonwelded rocks occur in the center of the potential repository block. Conversely, the Tiva Canyon Tuff thins to the north, conforms to the topography formed by older rocks, and is missing several areas in this region. Despite the significant thickness changes from north to south, some units exhibit consistent physical and hydrologic properties from Pagany Wash, south to Busted Butte (Istok and others, 1994).

METHODS

Sample-Collection Methods

Transects were located to sample all lithologic units exposed at Yucca Mountain (fig. 1), as well as to provide spatial coverage to assess the horizontal variability of several units. These comprised eight separate transects: five vertical transects, each covering several rock units, and three horizontal transects to evaluate the spatial variability of particular units. The location, length, number of samples, and general lithology for each transect are listed in table 1.

The vertical transects were located at (1) Solitario Canyon, at the southern end of the potential repository area, where the Tiva Canyon Tuff, bedded and nonwelded tuffs and upper Topopah Spring Tuff were sampled; (2) Busted Butte to the south, where the Topopah Spring Tuff was sampled; (3) Yucca Wash at the north end of Yucca Mountain, where the tuffs of the Paintbrush Group and Calico Hills Formation were sampled; (4) Windy Wash west of Yucca Mountain, where the entire section of the tuffaceous beds of Calico Hills were sampled; and (5) Pagany Wash, about three-fourths of the way up the wash, where the upper portion of the Tiva Canyon Tuff caprock (fig. 1) is preserved.

The horizontal transects of selected lithologic units were conducted at (1) Solitario Canyon, sampling the nonwelded base of the Tiva Canyon Tuff (shardy base); (2) Solitario Canyon, sampling the vitric caprock of the Topopah Spring Tuff; and (3) Yucca Crest, sampling the upper-cliff unit of the Tiva Canyon Tuff. The base of the Tiva Canyon Tuff is a zone that transitions from the densely welded tuffs to the underlying nonwelded and bedded tuffs. This unit (shardy base) is approximately 7–10 m thick throughout the potential repository region and grades from partially welded and 12–15 percent porosity to nonwelded and 50–55 percent porosity. It represents a stratigraphic feature that may form a hydrologic-flow barrier. This unit was sampled in detail and discussed by Istok and others (1994) and Rautman and others (1995). The vitric, densely welded caprock unit of the Topopah Spring Tuff (vitric caprock) is very thin, approximately 0.2 to 0.4 m thick, and seems to be laterally extensive over the entire study area. The unit has a porosity of 1 to 4 percent and underlies a high-porosity (40–60 percent) nonwelded tuff. It represents a lithologic discontinuity that may influence downward movement of water and result in lateral diversion. The rocks on the crest of Yucca Mountain belong to the upper-cliff unit of the Tiva Canyon Tuff, which changes in porosity from approximately 30 percent to 10 percent over a short vertical distance, so that erosion on the crest of the ridge has produced a slight north-south trend in porosity. Because this unit forms most of the exposed bedrock surface over the potential repository, it was important to characterize the material properties of this upper boundary on a north-south trend.

Sampling was performed using water and a hand-held, gas-powered drill with a 2.5-cm I.D. core bit. Field samples ranged from 3 to 10 cm long. Samples were placed in plastic bags and labeled with a transect identification and a sample number. This number was either the distance along the transect or a consecutive position value. Relative vertical sample positions were measured using a 1.5-m Jacob's staff and Brunton compass, and they were adjusted to true stratigraphic positions. Relative horizontal positions were measured in the field using a Topofil string measuring device or 30.5-m chain.

Laboratory Measurements

Cores were prepared for measurement in the laboratory by trimming the ends to a final core length of approximately 5 cm. If less core was obtained, the final size was kept as long as possible. All cores were labeled with a permanent ink marker. Core samples

Table 1. **Transects and their location, northing and easting according to Nevada State Plane Coordinate System, length, number of samples, and lithologic description**

[Vertical transects start at the listed location and extend downslope; horizontal transects start at the listed location and extend northward; m, meters]

Transect ID	Location description	Northing	Easting	Length (m)	Number of samples	Lithologic description
Solitario Canyon (vertical)	West side of crest, below USW UZ-6s.	231,650	170,140	315	169	Upper cliff zone of the Tiva Canyon Tuff to the top of the lower lithophysal zone of the Topopah Spring Tuff.
Busted Butte (vertical)	Northeast side of Busted Butte.	225,920	174,650	135	102	Upper nonwelded tuff of the Topopah Spring Tuff to the basal vitrophyre.
Yucca Wash (vertical)	South side of Yucca Wash.	238,660	168,550	290	139	Caprock of the Tiva Canyon Tuff through the Calico Hills Formation.
Pagany Wash (vertical)	Upper Pagany Wash, north-facing slope.	236,220	170,700	25	20	Caprock of the Tiva Canyon Tuff to the upper lithophysal zone.
Calico Hills (vertical)	Windy Wash, south-facing slope.	238,660	167,640	102	66	Calico Hills Formation and Prow Pass Tuff.
Yucca Crest (horizontal)	Crest of Yucca Mountain.	229,510	170,230	5,030	45	Upper cliff zone of the Tiva Canyon Tuff.
Shardy Base (horizontal)	West side of crest.	231,650	170,080	701	65	Nonwelded base of the Tiva Canyon Tuff.
Topopah Caprock (horizontal)	West side of crest.	231,340	170,080	1,823	50	Vitric caprock of the Topopah Spring Tuff.

were saturated with CO_2 after evacuation of air under a vacuum to enable the saturation of small internal pores and then submersed in distilled, de-aired water and left overnight. Samples were removed, dried with a damp towel (American Society of Testing Materials, 1977), and weighed to determine saturated weight. The sample was then suspended in a beaker of water in a wire basket to determine volume displacement and then dried in a relative humidity oven at 60°C and 45 percent relative humidity and reweighed. Relative-humidity drying removes water from the pores but retains water in the crystal or mineral structure (Bush and Jenkins, 1970). Hydrologic-flow properties were measured before conventional oven drying (105°C) because structural damage may occur in certain samples with delicate clay structures or zeolites. Finally the samples were dried at 105°C to obtain a standard dry weight.

A representative set of 41 samples was selected for additional measurements to form a composite vertical profile of all units. Imbibition tests were conducted on these samples to determine sorptivity at relative-humidity-dried saturations. Samples were weighed and placed on a wet towel saturated by using a Mariotte system with a constant head of zero. They were reweighed repeatedly, and times and weights were recorded in order to describe the quantity of water imbibed with time. When plotted as water imbibed versus the square root of time (t), early imbibition (I) is calculated as sorptivity (S) according to $I = St^{0.5}$ (Philip, 1957; Talsma, 1969).

After the imbibition tests, the samples were resaturated, and saturated hydraulic conductivity was determined on the same 41 samples using a steady-state permeameter that forces water through the core at a measured pressure while weighing the outflow with time. All samples were then dried at 105°C for 48 hours for final calculations. Porosity [(saturated weight-dry weight)/volume], bulk density (dry weight/volume), and particle density [porosity/(1-bulk density)] were calculated. Following these measurements, subsamples approximately 1 cm long were cut, and moisture-retention curves were determined for the subsamples using a chilled-mirror psychrometer (Model CX-2 Water Activity Meter, Decagon Devices, Inc., Pullman, Wash.) to determine water potential at various saturations. Each of the moisture-retention curves were fitted using (1) van Genuchten (1980) fitting α and n, while $m = n - 1/n$; (2) fitting α, n, and m; and (3) Brooks and Corey (1964). For the van Genuchten fits, residual water content was estimated from the difference between relative-humidity oven-dry weight and 105°C oven-dry weight.

RESULTS

Physical Properties

Trends in porosity and particle density are observed in each of the eight transects (figs. 3–10). The major flow units (Tiva Canyon and Topopah Spring Tuffs) are apparent in the Solitario Canyon transect (fig. 3), with high porosity zones at the top of each major flow unit and very high porosity zones in the nonwelded units of the Paintbrush Tuff (Ptn, Ortiz and others, 1985). Particle density follows similar trends in the welded units but is very low in the PTn. Samples from Busted Butte (fig. 4) show similar trends in properties in the Topopah Spring unit as those from Solitario Canyon, and porosity is very low, 2–3 percent, in the basal vitrophyre. The Yucca Wash vertical transect (fig. 5) extends from the top of the Tiva Canyon Tuff through the PTn, the Topopah Spring Tuff and the tuffaceous beds of Calico Hills Formation. There appears to be more scatter in the porosities of these cores, which is probably due to differences in welding. The Yucca Mountain and Pah Canyon Tuffs are present in the Yucca Wash transect, and the Yucca Mountain Tuff comprises a full suite of nonwelded to welded tuffs. Densely welded caprock of the Tiva Canyon Tuff occurs in this transect, and in the Pagany Wash transect (fig. 6). Low porosity values that increase rapidly with depth are recorded for samples from both of these transects. Most of the densely welded Tiva Canyon Tuff caprock has been eroded south of Drill Hole Wash (fig. 1), resulting in exposures of the more permeable lower caprock and upper-cliff zones. Zeolitized rock in the Calico Hills Formation (fig. 7) increase slightly in porosity with depth throughout the transect. Two samples of the Prow Pass Tuff of the Crater Flat Tuff are also present in the Calico Hills transect.

The horizontal transect on Yucca Crest was designed to investigate the properties of the upper cliff unit of the Tiva Canyon Tuff, which decreases in porosity with depth fairly rapidly (fig. 8). A regression analysis was performed on porosity with depth and showed a slight trend of decreasing porosity toward the south, where the surface of the mountain is eroded slightly more. The horizontal transect through the nonwelded shardy base of the Tiva Canyon Tuff (fig. 9), originally designed to investigate horizontal variability, actually identified vertical trends. Based on the data from the Solitario Canyon transect, the top of the unit is low in porosity (15 percent) and increases to about 55 percent porosity over a vertical distance of approximately 7 m. Any deviation in elevation during sampling, such as moving downslope due to topographic changes along the horizontal transect, resulted in a change in porosity. Comparison of the data with the vertical transect at Solitario Canyon indicates that the interpretation of the changes was due to the vertical porosity trend, rather than lateral variation. These trends were investigated by Istok and others (1995) with a series of 26 vertical transects through the unit to produce a 2-dimensional representation of porosity and permeability that supported interpretations of influences of deterministic processes on hydrologic properties and the interpretation of a small degree of horizontal variability, while the vertical variability, though large, was predictable. The transect along the exposure of the vitric top of the caprock of the Topopah Spring Tuff (fig. 10) was planned following the measurements of physical and hydrologic properties on samples from the Solitario Canyon transect. The porous PTn under this extremely low porosity, very thin unit (0.2–0.3 m), has been overlooked or averaged into larger units in several modeling exercises (Wittwer and others, 1992; Brown and others, 1994). The sampling of this unit exhibits some of the same problems associated with the sampling of the shardy base unit, that of rapid vertical change in porosity. There are several locations along this transect where the porosity exceeds 6 percent. These locations most likely indicate a deviation downslope from the upper contact of the unit rather than lateral variation.

All individual measurements for each core sample are listed in Appendix I, with all samples listed for each transect along with transect distance, physical properties, and hydrologic-flow properties. Not all measurements were obtained from all samples.

Descriptive statistics were calculated for porosity, bulk density, particle density, saturated hydraulic conductivity, and sorptivity for each unit sampled for all transects combined (table 2). The principal differences between units are due to the variation in welding, which most directly influences porosity. Another characteristic influencing porosity is secondary alteration. Mean porosity varies from 3 percent in the vitric caprock and basal vitrophyre of the Topopah Spring Tuff to as high as 52 percent in the bedded and pumice-fall tuffs. The variation in bulk density shows the inverse trend. Particle density varies from 2.56 g/cm^3 in the densely welded caprock of the Tiva Canyon Tuff to 2.31 g/cm^3 in the zeolitized part of the Calico Hills Formation. Particle density generally is fairly uniform for all the welded units and for the rocks that have somewhat lower densities in the nonwelded units.

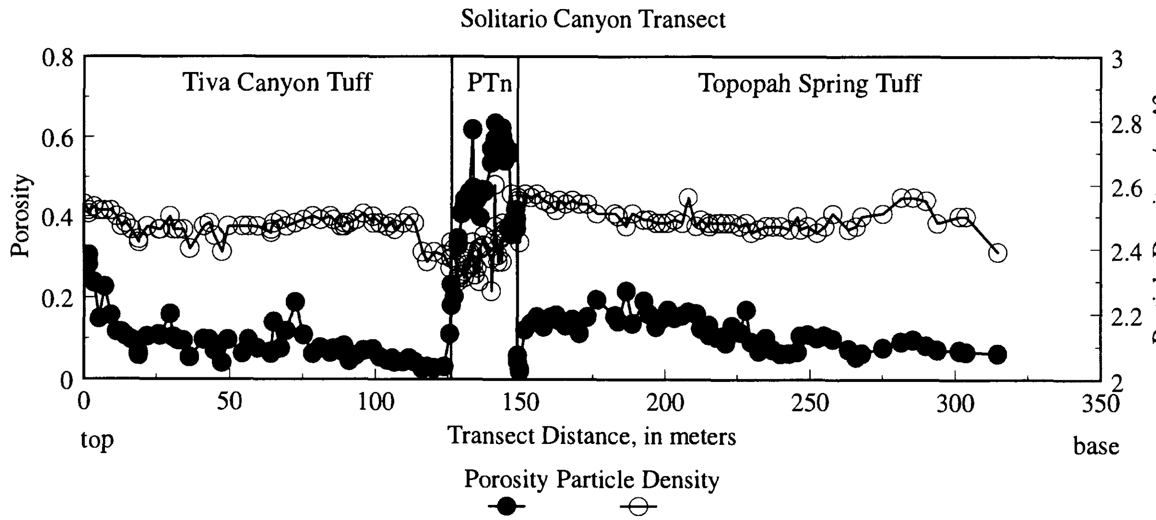

Figure 3. Porosity and particle density for core samples from Solitario Canyon vertical transect.

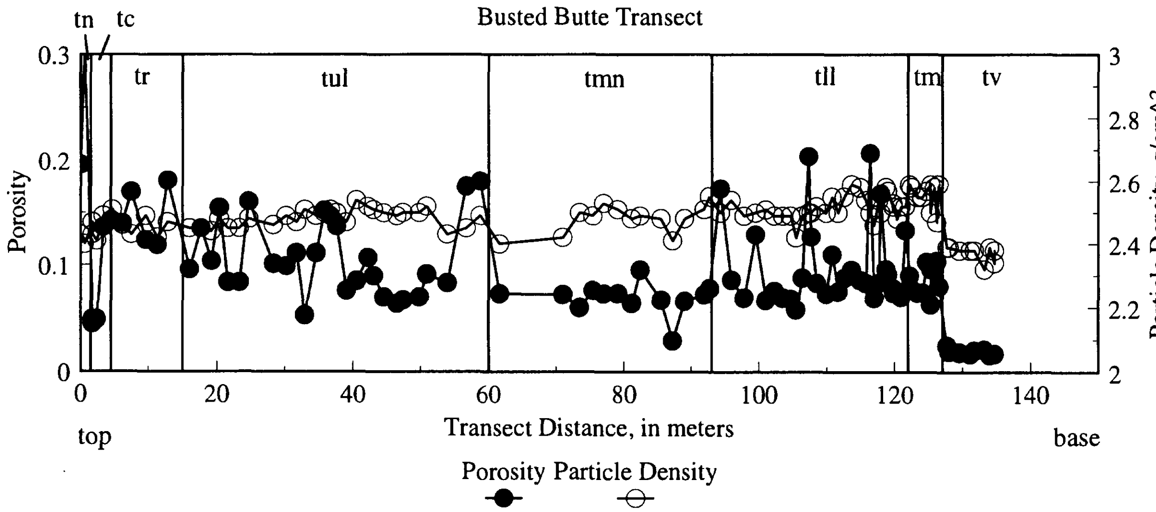

Figure 4. Porosity and particle density for core samples from Busted Butte vertical transect.

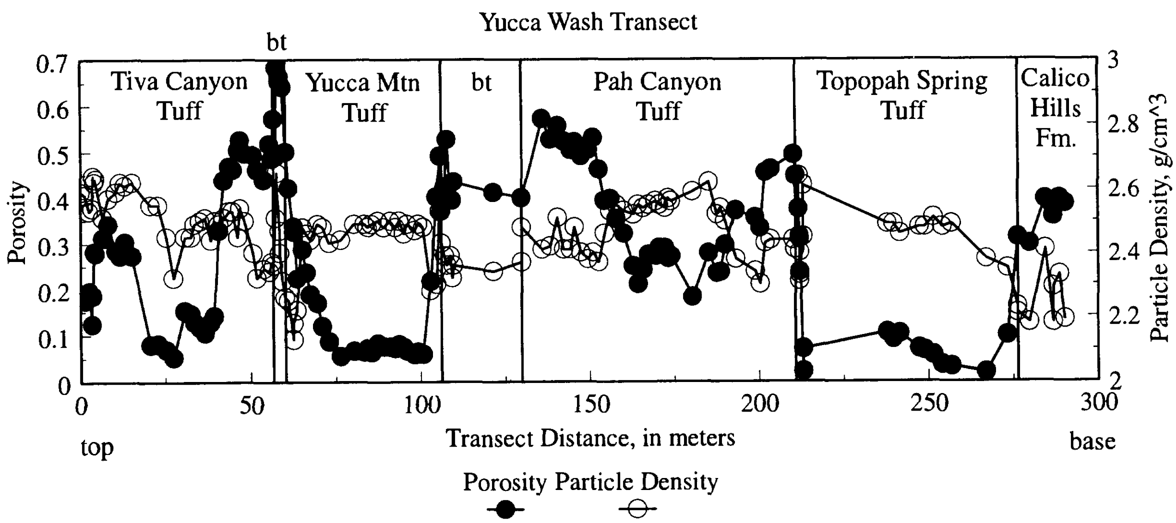

Figure 5. Porosity and particle density for core samples from Yucca Wash vertical transect.

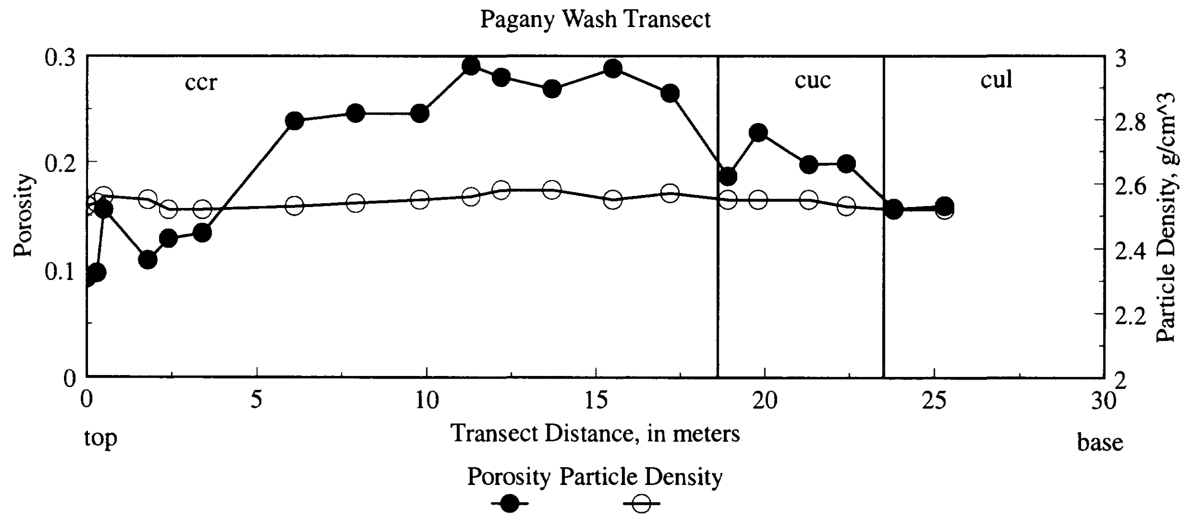

Figure 6. Porosity and particle density for core samples from Pagany Wash vertical transect.

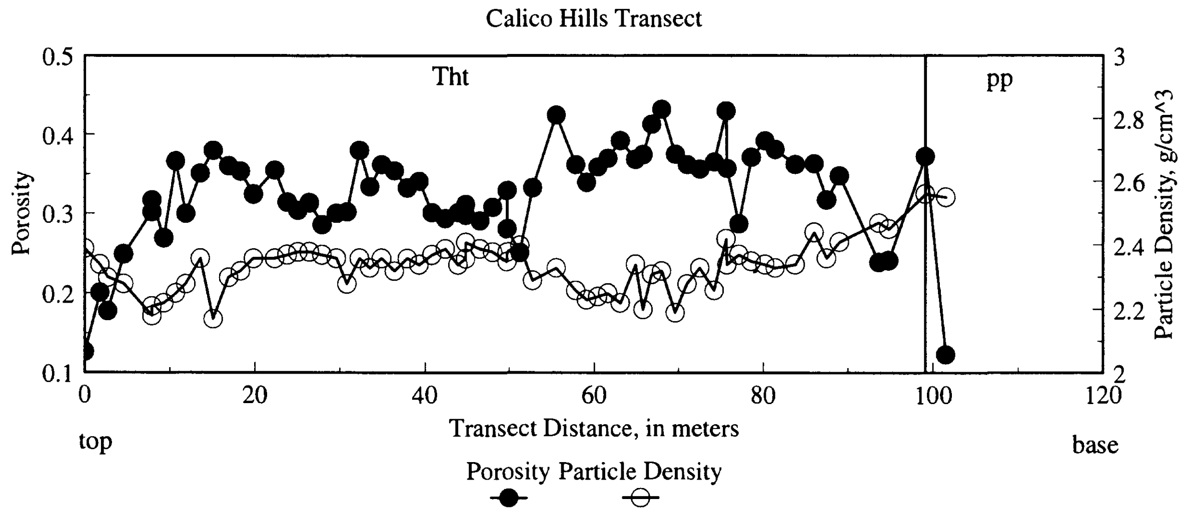

Figure 7. Porosity and particle density for core samples from Calico Hills Formation vertical transect.

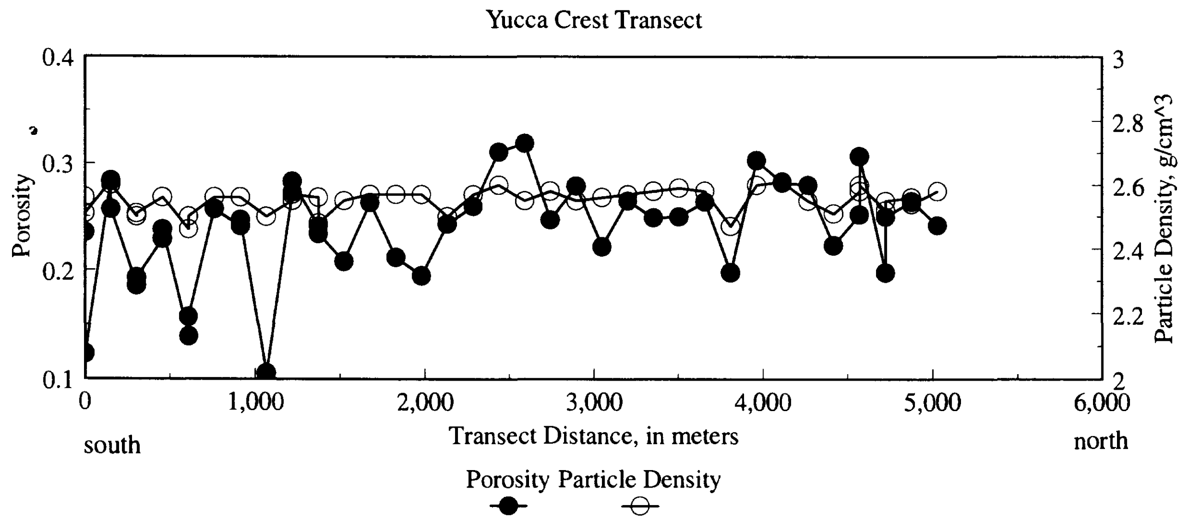

Figure 8. Porosity and particle density for core samples from Yucca Crest horizontal transect.

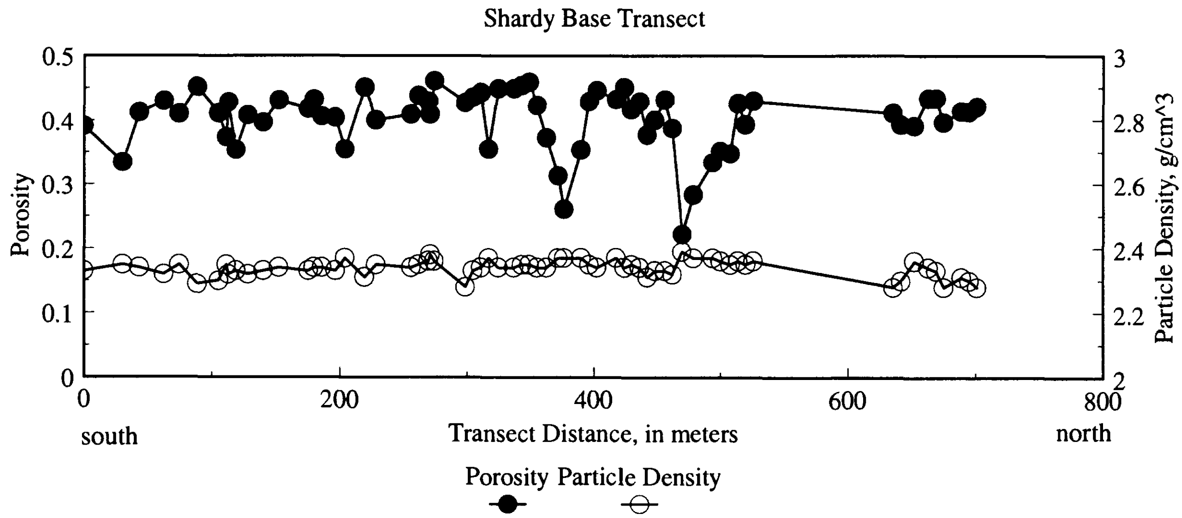

Figure 9. Porosity and particle density for core samples from shardy base horizontal transect.

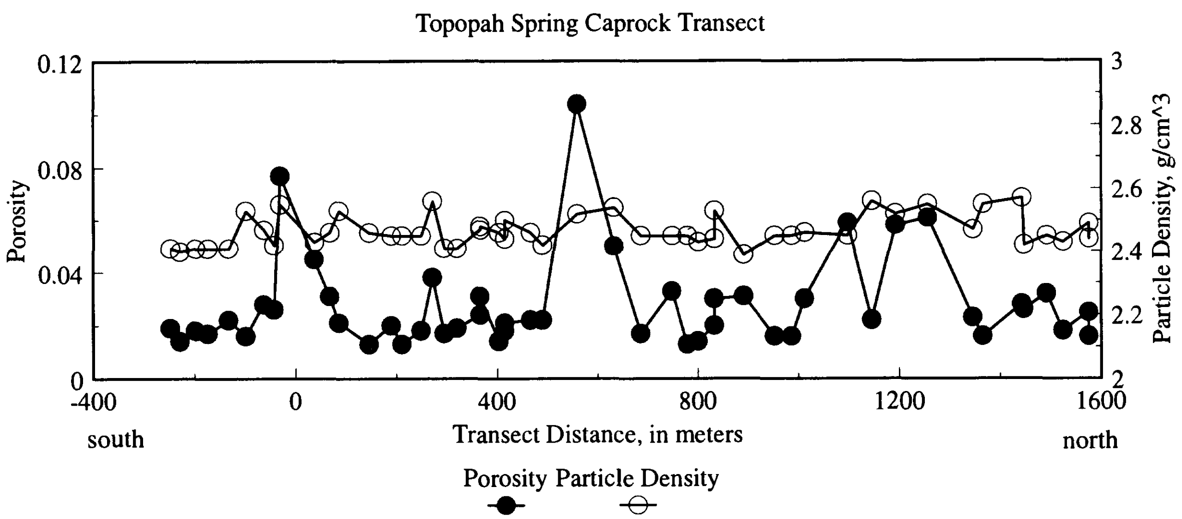

Figure 10. Porosity and particle density for core samples from Topopah Spring Tuff caprock horizontal transect.

Table 2. Descriptive statistics for each unit sampled for all transects for porosity, bulk density, and particle density calculated from 105°C oven-dry weights, and saturated hydraulic conductivity and sorptivity with number of samples

[cm^3/cm^3, cubic centimeter per cubic centimeter; g/cm^3, gram per cubic centimeter; m/s meter per second; N, number of samples; --, no data]

Unit sampled	Porosity (cm^3/cm^3)		Bulk density (g/cm^3)		Particle density (g/cm^3)			Saturated hydraulic conductivity (m/s)			Sorptivity ($m/s^{0.5}$)		
	Mean	Standard deviation	Mean	Standard deviation	Mean	Standard deviation	N	Mean	Standard deviation	N	Mean	Standard deviation	N
Tiva Canyon Tuff													
Caprock	0.22	0.07	1.99	0.18	2.56	0.03	27	3.1E-9	8.7	27	9.7E-6	--	1
Upper cliff	0.24	0.05	1.95	0.10	2.55	0.04	56	2.9E-9	1.0	56	9.7E-6	--	1
Upper lithophysal	0.11	0.03	2.20	0.04	2.47	0.03	11	8.9E-12	4.3	2	1.6E-6	1.7	2
Clinkstone	0.09	0.03	2.25	0.05	2.46	0.03	15	3.0E-12	1.1	3	1.3E-6	1.1	3
Lower lithophysal	0.09	0.03	2.28	0.09	2.49	0.02	17	1.0E-11	54.0	3	3.1E-6	1.1	3
Hackly	0.06	0.01	2.34	0.02	2.48	0.01	6	3.6E-12	--	1	1.2E-6	--	1
Columnar	0.08	0.05	2.25	0.10	2.44	0.06	15	2.1E-10	15.5	8	1.9E-6	2.8	2
Vitrophyre	0.07	0.04	2.20	0.11	2.36	0.02	2	4.5E-10	--	1	1.1E-6	--	1
Shardy base	0.41	0.11	1.39	0.25	2.37	0.08	30	1.6E-6	10.1	96	7.2E-5	4.5	9
Yucca Mountain Tuff													
Welded	0.06	0.01	2.32	0.02	2.47	0.01	15	--	--	0	--	--	0
Nonwelded	0.31	0.14	1.62	0.36	2.33	0.11	21	2.1E-7	13.8	13	1.5E-4	1.7	2
Pah Canyon Tuff													
Nonwelded	0.36	0.12	1.55	0.33	2.40	0.11	39	1.8E-8	48.3	36	3.9E-4	1.2	2
Bedded/pumice	0.52	0.10	1.13	0.24	2.37	0.10	23	5.9E-6	10.8	12	--	--	--
Topopah Spring Tuff													
Nonwelded	0.39	0.12	1.48	0.27	2.42	0.13	14	4.8E-7	5.6	6	1.0E-4	1.2	2
Vitric caprock	0.03	0.02	2.39	0.05	2.47	0.05	59	1.3E-9	--	1	1.5E-5	--	1
Caprock	0.10	0.03	2.24	0.06	2.49	0.02	11	5.4E-11	16.2	7	--	--	--
Rounded	0.14	0.02	2.16	0.06	2.52	0.04	16	1.3E-8	7.6	4	2.0E-5	1.1	3
Topopah Spring Tuff													
Upper lithophysal	0.12	0.04	2.19	0.10	2.48	0.02	60	2.1E-11	17.9	7	3.6E-6	2.0	7
Middle nonlithophysal	0.08	0.02	2.28	0.05	2.48	0.04	20	--	--	0	--	--	
Lower lithophysal	0.09	0.04	2.28	0.09	2.51	0.04	41	1.1E-12	2.8	2	3.8E-6	1.9	2
Lower nonlithophysal	0.05	0.02	2.36	0.04	2.49	0.01	5	1.5E-10	--	1	--	--	--
Mottled	0.09	0.01	2.34	0.05	2.56	0.04	10	3.1E-12	1.7	2	1.7E-6	1.2	2
Basal vitrophyre	0.03	0.03	2.33	0.09	2.41	0.06	18	3.0E-10	4.1	6	9.1E-7	--	1
Calico Hills Formation													
Nonwelded, zeolitized	0.33	0.05	1.54	0.12	2.31	0.10	62	7.9E-11	3.4	10	1.9E-5	1.4	4
Prow Pass Tuff													
Nonwelded	0.25	0.13	1.92	0.32	2.55	0.00	2	--	--	--	--	--	--

Hydrologic-Flow Properties

Saturated hydraulic conductivity (also referred to as conductivity) was not determined on very low-porosity samples with conductivities below 1E-12 m/s due to equipment limitations. This biases the calculation of mean conductivity when it is compared to other properties that were measured on many more samples. Conductivity ranged from 5.9E-6 m/s for bedded tuffs to 3.0E-12 m/s for the clinkstone unit of the Tiva Canyon Tuff.

Conductivity appears to be well correlated with the physical properties. Porosity of most of the tuffs may be of a similar nature, that is, pore structure and tortuosity. Some of the tuffs have alterations to the porosity, such as zeolites, which form in the flow channels of the highly porous Calico Hills Formation and reduce conductivity. Another difference is in vitric caprock and vitrophyre samples (vitrophyre), many of which have microfractures that contribute to saturated flow but do not represent a large enough volume to affect porosity. The relationship between measurements of conductivity and porosity is improved when porosity is calculated using relative-humidity-dried weights compared to when 105°C dry weights are used. This observation is attributed to the presence of clay minerals in some samples. These clays contain loosely bound structural water that is not available for flow. When dried in a high relative-humidity environment, water is removed from the flow channels but maintained in the minerals, thus allowing for more relevant flow-channel porosity determinations.

Nonlinear regression analyses were performed on porosity and conductivity values measured on samples from the Solitario Canyon transect and for samples from the Yucca Wash transect (table 3). A scatterplot of conductivity and porosity for the Solitario Canyon transect (fig. 11a) illustrates the separate grouping of the vitrophyre samples (vitric caprock of the Topopah Spring Tuff and vitrophyre of the Tiva Canyon Tuff). The regressions were done on lithologic groupings of samples in order to increase the predictive capability. Coefficients of determination (r^2) are high for the Solitario Canyon transect with $r^2 = 0.72$ for the vitric samples and $r^2 = 0.90$ for all remaining welded and nonwelded samples.

The Yucca Wash transect has a larger scatter of points due to the inclusion of the samples from the Calico Hills Formation and several samples of the Pah Canyon Tuff. The samples from the Calico Hills Formation contain large amounts of zeolites, but the Pah Canyon Tuff samples also appear to have high amounts of clay. This is suggested by the large difference in these samples between porosities calculated from relative humidity dry weights, which retains the water in clays, and 105°C oven-dry weights, which removes the water from the clays. These samples have high porosities, but the development of zeolites and clays within the pore channels restricts flow, thus changing the relationship between porosity and saturated hydraulic conductivity. The vitrophyre and vitric caprock samples, on the other hand, have higher conductivities than would be suggested by their very low porosities. These vitrophyre samples have a bimodal pore-size distribution (discussed in following section) with very low matrix porosity due to the vitrification but have small microfractures that transmit water yet contribute little

Table 3. Nonlinear regression analysis performed for porosity and saturated hydraulic conductivity for the Solitario Canyon transect and the Yucca Wash transect

[N, number of samples; r^2, coefficient of determination; K_s, saturated hydraulic conductivity; ϕ, porosity, calculated from relative-humidity drying]

Transect N lithology	Regression equation	r^2	
Solitario Canyon transect			
Welded and nonwelded	$K_s = -13.9 + 33.1\,\phi - 30.8\,\phi^2$	0.90	36
Vitric	$K_s = -7.4 - 56.6\,\phi + 417.6\,\phi^2$	0.72	6
Yucca Wash transect			
Welded and nonwelded	$K_s = 0.00009 - 0.0007\,\phi + 0.0012\,\phi^2$	0.39	100
Welded and nonwelded, no clays	$K_s = -11.9 + 18.1\,\phi - 10.7\,\phi^2$	0.77	88
Clay (Pah Canyon Tuff and Calico Hills Formation)	$K_s = -8.8 - 13.1\,\phi + 32.1\,\phi^2$	0.50	12
Calico Hills Formation	$K_s = 11.6 - 168.0\,\phi + 318.7\,\phi^2$	0.84	6
Vitric	$K_s = -9.1 - 40.8\,\phi + 506.9\,\phi^2$	0.28	7

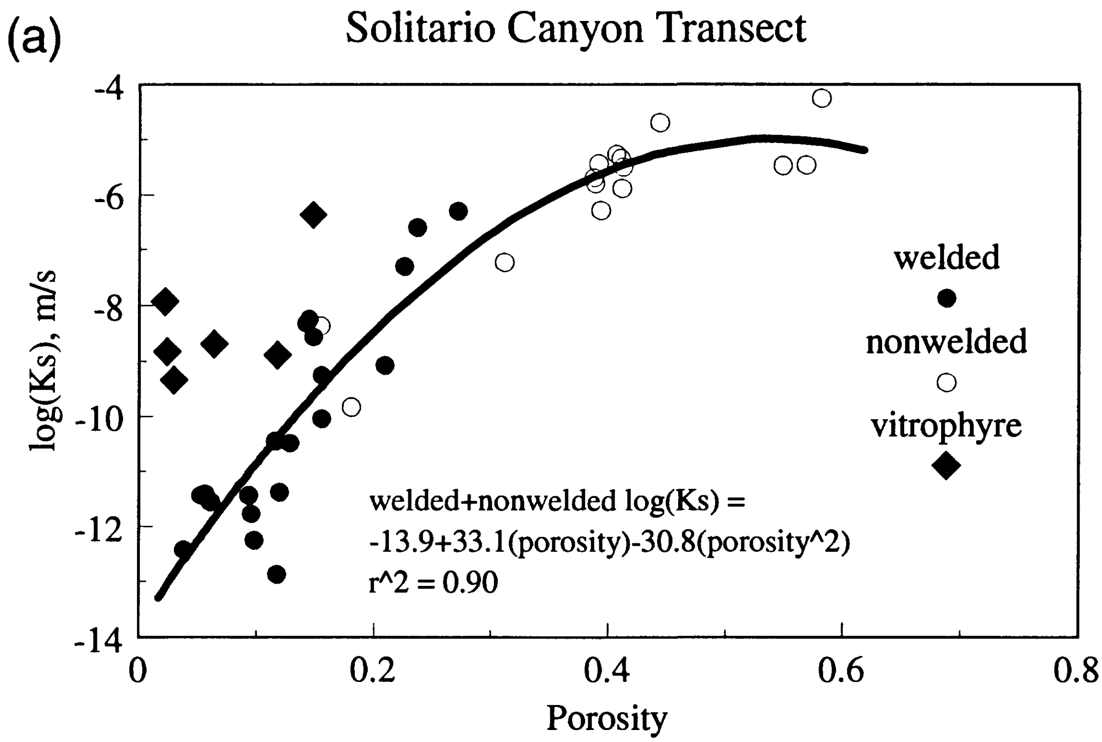

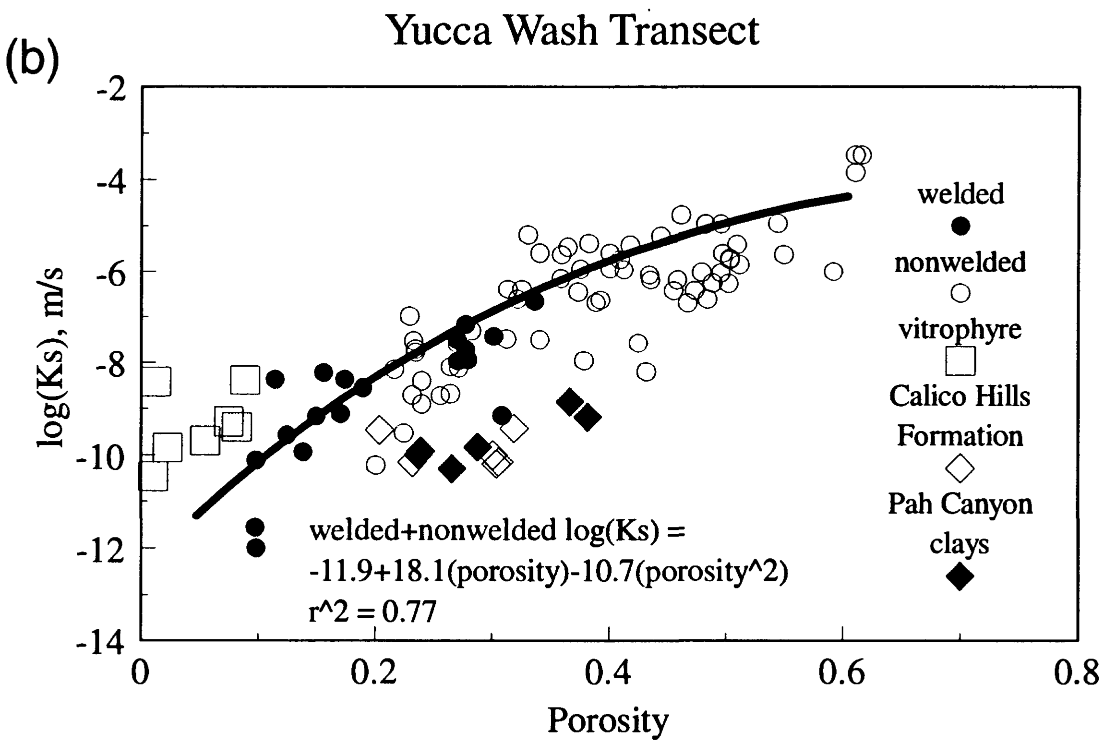

Figure 11. Relationship of porosity and saturated hydraulic conductivity for samples from (a) Solitario Canyon transect, and (b) Yucca Wash transect. Regression lines are for analyses on welded plus non-welded samples only.

to the porosity. Consequently, regression analyses were performed for several groupings of samples (fig. 11b). The samples from the Calico Hills Formation are analyzed separately (Calico Hills) and also along with the clayey samples from the Pah Canyon Tuff discussed above (Pah Canyon Tuff). The vitrophyre and vitric caprock samples are analyzed separately (vitrophyre). The remaining nonwelded samples combined with all the welded samples comprised the last regression analysis. For ease of presentation, only regression lines and equations for the welded plus nonwelded samples (not including those with high amounts of clays) are included on figures 11a and b, but all equations and r^2 values are listed in table 3. There are some differences between the regression equations developed using samples from the two transects. These differences may represent influences of lateral spatial variability on the relationship between porosity and conductivity. The differences more likely are due to the much thicker PTn present to the north in the Yucca Wash transect and the larger range in porosity, as well as the inclusion of the samples of the welded parts of the Pah Canyon and Yucca Mountain Tuffs. For these two transects, the most significant relationships between conductivity and porosity occur in the welded and nonwelded samples, not including samples with clays or vitric samples.

Sorptivity was determined for many fewer samples than conductivity and has a narrower range in values between units. The trends are similar for both measurements though with lower sorptivity in the welded units and the highest values in the nonwelded units.

Estimates of Hydrologic Units for Flow Modeling

Many of the lithologic units reflect predictable hydrologic and physical properties; however, some of these properties are not bounded by lithostratigraphic contacts. This is noticeably true in the upper Tiva Canyon Tuff where the caprock unit grades downward from densely welded to moderately welded tuff and is underlain by the upper cliff zone that is moderately welded tuff at the top and changes rapidly with depth to densely welded tuff. The references to welding in this paper are loosely characterized, however, and primarily infer a relationship with rock density. More current thought suggests that many of the rocks initially characterized as moderately welded are actually welded to densely welded but have a reduced density due to secondary alteration of the pores (C.A. Rautman, Sandia National Laboratory, personal commun., 1994). This example prompts the use of welding character rather than lithologic description and contacts to define hydrogeologic units with similar hydrologic properties and a reduction in variation within the unit.

To compile a complete set of data to accurately represent the means of each unit present in the unsaturated zone (table 4), the saturated hydraulic-conductivity data were extended to include estimates of conductivity for those samples upon which measurements could not be taken because of extremely low flow rates. Estimates of conductivity were made for densely welded samples using the regression for welded plus nonwelded samples from figure 11a for the Solitario Canyon transect. This should more accurately reflect properties of the potential repository block than the Yucca Wash transect regressions. These estimates are included with measured data in calculations of mean and standard deviation for each hydrogeologic unit. The stratified nature of each of the major flow units is maintained, and the Tiva Canyon Tuff is divided into densely welded caprock, moderately welded units, and welded units. All nonwelded tuffs from the Paintbrush Group are in one unit, and the calculations of the Topopah Spring Tuff include welded rocks with and without incorporating highly vitric samples. The Calico Hills Formation samples and Prow Pass Tuff samples are maintained separately because of the lack of data for samples from the Prow Pass unit, and therefore, no evidence supports combining the units.

This approach reduces the standard deviation of property values within hydrogeologic units and more accurately represents the changes with depth that occur. The surface of Yucca Mountain is variably covered by the three Tiva Canyon units due to weathering and erosion (Flint and Flint, 1994). This is significant in the construction of hydrologic models because the surface unit will control the upper boundary conditions for infiltration at all locations. The weak point in this approach is in combining the nonwelded units of the Paintbrush Group that vary laterally in thickness, as well as including very thin layers that may or may not be laterally extensive. The rapid changes in physical properties with depth that occur, especially in the nonwelded base of the Tiva Canyon Tuff, as well as the intervening bedded and ash-fall tuffs, need to be described for each location to adequately describe the hydrologic character for a flow model. An additional problem with this approach is the exclusion of the more welded Yucca Mountain Tuff that is located north of the potential repository location. This welded unit appears to be absent within the potential repository block itself, which could reduce the impact of this omission and probably only restrict the user to smaller

Table 4. Descriptive statistics for all transects, combining lithology into hydrogeologic units for porosity, bulk density, and particle density calculated from 105°C oven-dry weights, and saturated hydraulic conductivity and sorptivity with number of samples

[Saturated hydraulic conductivity is calculated using both measured values and estimates from regression with porosity; cm^3/cm^3, cubic centimeter per cubic centimeter; g/cm^3, gram per cubic centimeter; m/s, meter per second; N, number of samples; --, no data]

Hydrogeologic unit	Porosity (cm^3/cm^3)		Bulk density (g/cm^3)		Particle density (g/cm^3)			Saturated hydraulic conductivity (m/s)			Sorptivity ($m/s^{0.5}$)		
	Mean	Standard deviation	Mean	Standard deviation	Mean	Standard deviation	N	Mean	Standard deviation	N	Mean	Standard deviation	N
Tiva Canyon Tuff													
Densely welded caprock	0.12	0.02	2.23	0.06	2.54	0.02	6	1.1E-10	1.9	6	9.7E-6	--	1
Moderately welded	0.25	0.04	1.92	0.10	2.56	0.03	71	5.1E-9	3.4	71	9.7E-6	--	1
Welded	0.09	0.04	2.25	0.08	2.47	0.04	64	8.2E-12	14.1	62	1.8E-6	1.9	11
Paintbrush Group Nonwelded	0.41	0.13	1.42	0.34	2.42	0.10	129	5.7E-7	32.1	201	1.0E-4	3.7	15
Topopah Spring Tuff Welded	0.08	0.05	2.28	0.11	2.48	0.05	240	3.2E-11	18.7	96	4.5E-6	2.8	16
Welded, no vitric caprock or vitrophyre	0.11	0.04	2.24	0.10	2.50	0.04	163	2.9E-11	16.6	80	4.7E-6	2.7	14
Calico Hills Formation Nonwelded zeolitized	0.33	0.05	1.54	0.12	2.31	0.10	62	1.0E-10	3.5	12	1.9E-5	1.4	4
Prow Pass Tuff Nonwelded	0.25	0.13	1.92	0.32	2.55	0.00	2	--	--	--	--	--	--

scale hydrologic modeling. Alternatively, this unit may be very important in light of flux estimates made by Flint and Flint (1994), suggesting that the tuffs in the northern portions of the site have much higher surface fluxes than those over the repository block due to downcutting of the washes, which exposes the higher porosity PTn at the surface. As high flux boundary conditions correspond to surface exposures of the PTn, a detailed geometry of the site and the inclusion of welded tuffs within the thick PTn to the north are critical information when flow models are being developed. In any case, this set of calculations provides a substantial improvement over the data sets used in simplified models that have predominated in the past (Nitao and others, 1992; Montazer and Wilson, 1984) and primarily adds the distinction of the variably welded Tiva Canyon Tuff, which is exposed at varying elevations in the flow unit over the surface of the site.

Moisture Retention

The results of the moisture-retention characterization are tabulated in table 5, with bulk density and porosity for the subsample (denoted as the sample ID from the original core plus an "s"). Included are residual water-content estimates from the original sample that were used in the van Genuchten parameter modeling. The moisture-retention data are tabulated in Appendix II and are plotted with the three models fit to the data for each of the 41 core samples in Appendix III.

The two van Genuchten models generally fit the data very well. The three-parameter (estimated *m*) estimation model was not very different from the two-parameter (calculated *m*) model but in some cases fit the air-entry section of the data slightly better. The Brooks and Corey model fit many of the curves very well, but when it did not match, it generally underpredicted the wet end of the curve relative to the van Genuchten models. In general, the van Genuchten alpha parameter (approximately equal to the reciprocal of the air-entry pressure) increased as the porosity decreased, with the result that the welded samples have higher alpha values. This tendency was not observed for samples of Topopah Spring Tuff vitric caprock (BT1s and BT2s), which tended to lose water from the microfractures as the core dried and resulted in a higher alpha parameter. The data for BT1s may indicate a possible double-peak curve, which might describe a separate curve for fractures and matrix. Alternatively, the Tiva Canyon Tuff vitrophyre samples had extremely low alpha values and very high air-entry pressures. The resolution of the chilled-mirror psychrometer is plus or minus 0.13 MPa, however, and the description of air entry using the data may be slightly in error. The types of rocks in which the three models differed the most are the very low-porosity welded samples and the high-porosity samples with many larger pores that resulted in plots with a very flat slope at the wet end of the curve.

Relationships of porosity versus van Genuchten parameters were examined as a possible surrogate to intensive laboratory measurements (figs. 12a and b), and simple linear regressions were developed (table 6) for predictive purposes. For predictive purposes and considering the variability of *n* for all samples, porosity is fairly well related to *n* for nonwelded samples ($r^2 = 0.44$), while the welded samples have a narrow range of porosity and a larger range for α and *n* that reduces predictive capabilities. This interpretation is also made in light of the study done by Glass and others (1994) that used regressions of porosity and van Genuchten parameters to predict parameters for modeling flow through a slab of Topopah Spring Tuff that had many measurements of porosity. Their relationships between porosity and van Genuchten parameters did not appear to be very good (no r^2 value was included in the paper) yet moisture-retention curves generated from the best and worst case predictions were very similar. The Calico Hills Formation zeolitized samples also have a narrow range of porosity; but whereas α has a large range, *n* is clustered around 1.2, so despite the high r^2 value (0.98), the predictive value is low. While the relationship of porosity to permeability shown in figures 11a and b shows similarity for all the vitrophyre samples (includes both vitric caprock and vitrophyre), the data for the α parameter suggest some differences. All vitrophyre samples have very low porosity but air entry (approximately 1/ van Genuchten α, and equal to Brooks and Corey α) is low for the two Topopah Spring Tuff vitric caprock samples, whereas it is high for the Tiva Canyon and Topopah Spring Tuff vitrophyre samples. This indicates that the size of the microfractures may be larger for the caprock samples. The similarity of saturated hydraulic conductivities for these samples, however, suggests that the microfractures in the vitrophyre samples, while having an air- entry value near zero, will fill with water under a positive head, as done during a permeability measurement (or, for that matter, under a perched water body, in tuffs exposed at the surface, or during fracture flow) and contribute to higher flow rates. This may also suggest that the high permeability of these samples is due more to a lack of tortuosity of the microfractures rather than the larger size relative to pores. An implication of the difference in air entry and the similarity in saturated

Table 5. Properties and moisture-retention characteristics for subsamples from outcrop transect samples

[Modeling parameters were generated using van Genuchten and Brooks and Corey equations; van Genuchten curve fit parameters are modeled for alpha (α), n and m (m est), and α and n only (m calc, where $m = 1 - 1/n$); residual water content is theta (r); g/cm^3, gram per cubic centimeter; cm^3/cm^3, cubic centimeter per cubic centimeter; MPa, megapascals]

Unit sampled	Sample ID	Bulk density (g/cm^3)	Porosity (cm^3/cm^3)	Theta (r) (cm^3/cm^3)	van Genuchten						Brooks and Corey	
					Modeled 2 parameters			Modeled 3 parameters				
					α (est) (MPa^{-1})	n (est)	m (calc)	α (est) (MPa^{-1})	n (est)	m (calc)	α (MPa)	Slope
Tiva Canyon Tuff												
Caprock	PW19s	2.305	0.105	0.002	5.00	1.430	0.301	7.20	3.500	0.115	0.204	-2.418
Upper lithophysal	TPC52s	2.220	0.108	0.001	2.90	1.450	0.310	2.50	1.700	0.250	0.204	-2.418
Clinkstone	TPC35s	2.278	0.081	0.003	2.50	1.400	0.286	4.00	3.900	0.080	0.265	-2.760
Lower lithophysal	TPC27s	2.218	0.115	0.001	1.35	1.800	0.444	1.30	1.900	0.370	0.198	-2.204
Lower lithophysal	TPC15s	2.383	0.083	0.002	2.50	1.350	0.259	0.60	0.900	0.600	0.320	-2.703
Hackly	TPC9s	2.388	0.032	0.002	1.70	1.429	0.300	0.09	1.100	0.650	0.411	-4.190
Vitrophyre	TPC5s	2.325	0.035	0.001	0.90	1.254	0.203	0.07	0.900	0.380	0.341	-9.667
Vitrophyre	TPC2s	2.309	0.042	0.005	3.10	1.193	0.162	0.10	0.900	0.400	0.202	-10.728
Vitrophyre	TPC1s	2.127	0.120	0.001	1.35	1.250	0.200	0.37	0.900	0.400	0.490	-4.238
Shardy base	BT27Hs	1.944	0.208	0.010	1.77	1.230	0.187	3.00	1.100	0.220	0.214	-4.734
Shardy base	BT26Hs	1.849	0.235	0.035	3.01	1.310	0.237	0.98	1.128	0.600	0.095	-4.170
Shardy base	BT25Hs	1.556	0.346	0.010	12.21	1.333	0.250	3.00	1.000	0.600	0.043	-3.411
Tiva Canyon Tuff												
Shardy base	BT24Hs	1.378	0.406	0.030	4.27	2.062	0.515	5.00	14.000	0.050	0.053	-2.479
Shardy base	BT23-1Hs	1.368	0.412	0.010	13.71	1.476	0.322	7.00	3.300	0.200	0.034	-2.598
Shardy base	BT22Hs	1.360	0.425	0.050	6.35	2.067	0.516	9.46	17.000	0.050	0.032	-3.169
Yucca Mountain Tuff	BT18Hs	1.310	0.442	0.020	4.59	1.942	0.485	7.00	20.000	0.045	0.047	-2.748
Yucca Mountain Tuff	BT17s	1.614	0.442	0.030	3.94	1.716	0.417	5.00	14.000	0.050	0.066	-2.694
Pah Canyon Tuff	BT11s	0.861	0.628	0.030	3.78	1.923	0.480	7.00	20.000	0.045	0.068	-2.054
Topopah Spring Tuff												
Nonwelded	BT3Vs	1.615	0.381	0.015	8.00	2.048	0.512	10.00	10.000	0.100	0.033	-1.951
Caprock, vitric	BT2s	2.439	0.063	0.003	24.15	1.225	0.184	20.00	6.000	0.040	0.030	-4.492
Caprock, vitric	BT1s	2.456	0.045	0.008	23.69	1.173	0.147	6.00	1.100	0.272	0.028	-6.077
Caprock, devitrified	TS58s	2.279	0.124	0.003	8.97	1.363	0.266	10.00	6.000	0.070	0.043	-3.616
Caprock, devitrified	TS56s	2.130	0.184	0.007	11.15	1.389	0.280	8.00	12.000	0.050	0.050	-2.830

Table 5. Properties and moisture-retention characteristics for subsamples from outcrop transect samples--Continued

Unit sampled	Sample ID	Bulk density (g/cm^3)	Porosity (cm^3/cm^3)	Theta (r) (cm^3/cm^3)	van Genuchten						Brooks and Corey	
					Modeled 2 parameters			Modeled 3 parameters				
					α (est) (MPa^{-1})	*n* (est)	*m* (calc)	α (est) (MPa^{-1})	*n* (est)	*m* (calc)	α (MPa)	Slope
Topopah Spring Tuff												
Rounded	TS54s	2.258	0.120	0.008	7.68	1.383	0.277	4.00	2.000	0.280	0.066	-3.014
Rounded	TS50s	2.092	0.181	0.007	4.03	1.850	0.459	4.78	15.000	0.050	0.102	-2.254
Rounded	TS47s	2.077	0.185	0.005	2.37	2.204	0.546	2.80	4.500	0.200	0.097	-2.192
Upper lithophysal	TS40s	2.157	0.156	0.008	4.15	1.536	0.349	5.00	7.000	0.080	0.086	-2.538
Upper lithophysal	TS32s	2.207	0.115	0.008	2.81	1.314	0.239	2.80	5.000	0.080	0.211	-2.939
Upper lithophysal	TS29s	2.138	0.140	0.010	3.47	1.513	0.339	3.50	6.000	0.100	0.109	-2.709
Upper lithophysal	TS26s	2.180	0.129	0.010	6.48	1.401	0.286	3.40	2.500	0.240	0.059	-3.313
Upper lithophysal	BB68s	2.322	0.078	0.010	0.65	1.384	0.277	0.80	1.500	0.300	0.171	-5.032
Upper lithophysal	BB64s	2.023	0.192	0.010	2.24	1.575	0.365	1.40	2.000	0.360	0.144	-2.227
Lower lithophysal	BB45s	2.171	0.141	0.005	3.17	1.309	0.236	1.80	1.400	0.360	0.144	-3.44
Lower lithophysal	BB31s	2.324	0.099	0.005	5.52	1.361	0.265	1.80	1.400	0.360	0.115	-2.730
Mottled	BB16s	2.199	0.069	0.005	1.35	1.296	0.228	1.20	1.000	0.360	0.383	-3.228
Topopah Spring Tuff												
Mottled	BB13As	2.329	0.079	0.009	2.10	1.447	0.309	2.50	6.000	0.106	0.115	-3.254
Basal vitrophyre	BB5s	2.328	0.022	0.004	0.03	1.755	0.430	0.02	1.300	0.600	0.914	-5.174
Calico Hills Formation												
Zeolitized	CH60s	1.454	0.357	0.015	28.14	1.184	0.155	6.00	1.700	0.190	0.047	-4.253
Zeolitized	CH47s	1.632	0.322	0.070	5.18	1.147	0.128	3.00	1.100	0.220	0.071	-7.944
Zeolitized	CH44s	1.580	0.337	0.005	14.05	1.160	0.138	11.00	1.800	0.160	0.110	-3.852
Zeolitized	CH40s	1.427	0.401	0.090	9.51	1.211	0.174	10.00	9.000	0.040	0.046	-5.815

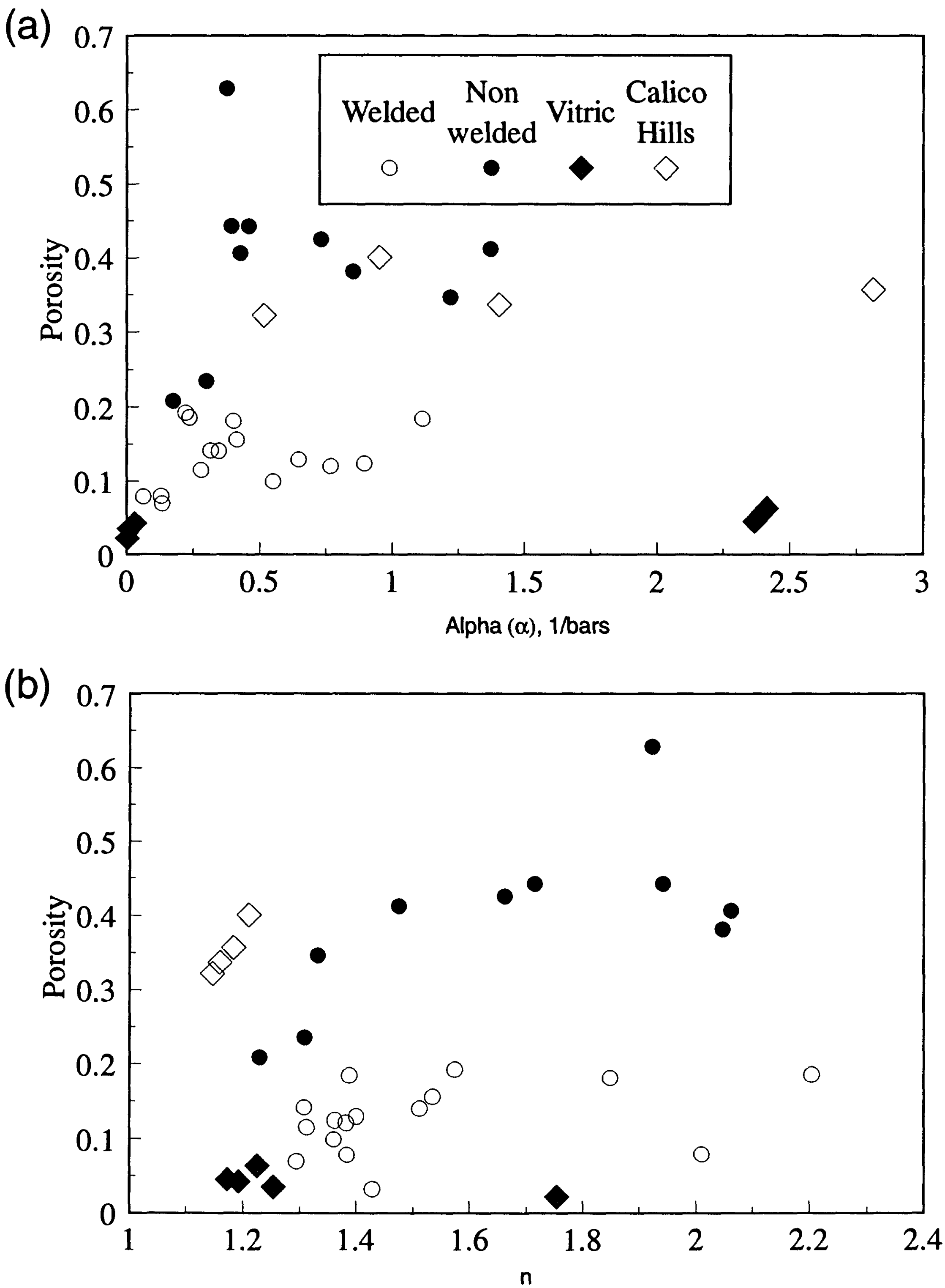

Figure 12. Relationship of porosity and van Genuchten parameters for (a) Alpha (α), and (b) *n*, for subsamples from 41 transect samples.

hydraulic conductivity may be that in 1-dimensional modeling of flow through these units, water is more likely to enter the vitric caprock under unsaturated conditions, whereas higher saturations may be necessary for flow to occur through the Tiva Canyon and Topopah Spring Tuff vitrophyres.

Table 6. Linear regressions of van Genuchten α and n parameters versus porosity for welded, nonwelded, vitrophyre, and Calico Hills Formation samples

[r^2, coefficient of determination; N, number of samples; ϕ, porosity]

Sample	Regression equation	r^2	N
Welded	$\alpha = 0.032 + 2.87\ (\phi)$	0.20	20
	$n = 1.17 + 2.66\ (\phi)$	0.20	20
Nonwelded	$\alpha = 0.49 + 0.31\ (\phi)$	0.01	10
	$n = 0.95 + 1.94\ (\phi)$	0.44	10
Calico Hills Formation	$\alpha = 0.29 + 3.19\ (\phi)$	0.01	4
	$n = 0.89 + 0.81\ (\phi)$	0.98	4
Vitrophyre	$\alpha = 0.84 - 0.96\ (\phi)$	0.01	7
	$n = 1.40 - 1.21\ (\phi)$	0.05	7

SUMMARY AND CONCLUSIONS

A set of data has been provided that includes physical- and hydrologic-flow property measurements on surface-outcrop samples from most of the rock units at Yucca Mountain. Observed porosity values range from 2 to 60 percent, and saturated hydraulic-conductivity values range from 1E-12 to 4E-6 m/s. The porosity range is much smaller within a lithologic unit. However, large variations may occur over very short vertical distances in the shardy-base subunit of the Tiva Canyon Tuff. In this unit, porosity changes from 15 percent to 55 percent within about 7.3 m. Another example is the transition zone in the upper Topopah Spring Tuff, where the vitric caprock (4-percent porosity) changes abruptly to nonwelded tuff (39-percent porosity) over a vertical distance of a few centimeters. It is apparent that there are many subunits with distinct properties that could affect the estimation of ground-water flow through the unsaturated zone.

Porosity appears to be a reasonable surrogate or estimator for saturated hydraulic conductivity and possibly van Genuchten moisture-retention parameters for the welded and nonwelded tuffs. These relationships are different for the tuffs with higher water-holding capacity such as zeolitized Calico Hills Formation tuff and some of the nonwelded units that retain large volumes of water when dried under relative-humidity conditions. The relationship is also different for densely welded, highly vitric samples such as the vitric caprock or vitrophyres that have microfractures. These relationships appear to be useful for estimating properties and parameters for modeling water flow in the absence of complete data sets.

Previous hydrologic modeling efforts have used data from a few samples to devise parameters for models that consist of relatively few layers such as the Tiva Canyon Tuff, the bedded and nonwelded units of the Paintbrush Group, the Topopah Spring Tuff, and the tuffs of the Calico Hills Formation. The data in this report describe many subtleties and rapid gradational changes within these generalized hydrogeologic-flow units. These differences may require substantially more layers to adequately model water flow. Major geologic boundaries do not always reflect hydrologic differences, as in the upper Tiva Canyon Tuff welded and moderately welded units. The existence of very rapid vertical changes will probably require 2-dimensional or 3-dimensional models in several locations to predict the likely occurrence of lateral diversions of flow.

Although there have been some successful comparisons between properties measured on surface outcrop samples and those from borehole samples, it is generally not possible to collect both types of samples in the same location. Additionally, there is inherent lateral variability between sampling locations. Therefore, these samples may not represent the true physical and hydrologic property values that exist in the subsurface. However, there also have been studies that indicate that formation saturations throughout the unsaturated zone can be predicted using model parameters characterized from outcrop samples. Despite the limitations inherent in an outcrop study, there is little question that there is significant vertical, and much less lateral variability of physical and hydrologic properties at Yucca Mountain.

REFERENCES

American Society of Testing Materials, 1977, Adsorption and bulk specific gravity of natural building stone: American Society of Testing Materials, ANSI/ASTM R97-47 Annual Book of ASTM Standards, part 19.

Brooks, R.H., and Corey, A.T., 1964, Hydraulic properties of porous media: Fort Collins, Colorado State University, Hydrology Paper 3.

Brown, T.P., Lehman, L.L., Nieber, J.L., 1994, Testing conceptual unsaturated zone models for Yucca Mountain: Proceedings International High-Level Radioactive Waste Conference, Las Vegas, Nevada, May 22–26, 1994, p. 1999–2006.

Buesch, D.C., Spengler, R.W., Moyer, T.C., and Geslin, J.K., (1996), Proposed revised stratigraphic nomenclature and macroscopic identification of lithostratigraphic units of the Paintbrush Group exposed at Yucca Mountain, Nevada: U.S. Geological Survey Open-File Report 94-469.

Bush, D.C., and Jenkins, R.E., 1970, Proper hydration of clays for rock property determinations: Journal of Petroleum Technology, v. 22, no. 7, p. 800–804.

Flint, A.L., and Flint, L.E., 1994, Spatial distribution of potential near-surface moisture flux at Yucca Mountain: Proceedings International High-Level Radioactive Waste Conference, Las Vegas, Nevada, May 22–26, 1994.

Flint, A.L., Flint, L.E., and Hevesi, J.A., 1993, Influence of long term climate change on net infiltration at Yucca Mountain, Nevada: Proceedings International High-Level Radioactive Waste Conference, Las Vegas, Nevada, April 25–30, 1993.

Glass, R.J., Flint, A.L., Tidwell, V.C., Peplinski, W., Castro, Y., 1994, Fracture-matrix interaction in Topopah Spring tuff—Experiment and numerical simulation: Proceedings International High-Level Radio active Waste Conference, Las Vegas, Nevada, May 22–26, 1994.

Istok, J.D., Rautman, C.A., Flint, L.E., and Flint, A.L., 1994, Spatial variability in hydrologic properties of a volcanic tuff: Ground Water, v. 32, no. 5, p. 751–60.

Montazer, P., and Wilson, W.E., 1984, Conceptual hydrologic model of flow in the unsaturated zone, Yucca Mountain, Nevada: U.S. Geological Survey Water-Resources Investigations Report 84-4345, 55 pp.

Nitao, J.J., Buscheck, T.A., Chestnut, D.A., 1992, The implications of episodic nonequilibrium fracture-matrix flow on site suitability and total site performance: Proceedings International High-Level Radioactive Waste Conference, Las Vegas, Nevada, April 12–16, 1992, p. 279–296.

Ortiz, T.S., Williams, R.L., Nimick, F.B., Whittet, B.C., and South, D.L., 1985, A three-dimensional model of reference thermal/mechanical and hydrological stratigraphy at Yucca Mountain, southern Nevada: Albuquerque, N. Mex., Sandia National Laboratories, SAND84-1076, 76 p.

Philip, J.R., 1957, The theory of infiltration 4. Sorptivity and algebraic infiltration equations: Soil Science, v. 84, p. 257–264.

Rautman, C.A., and Flint, A.L., 1992, Deterministic processes and stochastic modeling: Albuquerque, N. Mex., Sandia National Laboratories, SAND91-1925C.

Rautman, C.A., Flint, L.E., Flint, A.L., and Istok, J.D., Physical and hydrologic properties of outcrop samples from a nonwelded to welded tuff transition, Yucca Mountain, Nevada: U.S. Geological Survey Water-Resources Investigations Report 95-4061.

Sawyer, D.A., Flock, R.J., Lanphere, M.A., Warren, R.G., Broxton, D.E., and Hudson, M.R., 1994, Episodic calern volcanisms in the Miocene southwestern Nevada volcanic field—Revised stratigraphic framework, $^{40}Ar/^{39}Ar$ geochronology, and implications for magmatism and extension: Geologic Society American Bulletin, v. 106, no. N, p. 1304–1318.

Scott, R.B., and Bonk, J., 1984, Preliminary geologic map of Yucca Mountain with geologic sections, Nye County, Nevada: U.S. Geological Survey Open-File Report 84-494, scale 1:12,000.

Talsma, T., 1969, In-situ measurement of sorptivity: Australian Journal of Soil Research, v. 7, p. 269–276.

van Genuchten, M.Th., 1980, A closed-form equation for predicting the hydraulic conductivity of unsaturated soils: Soil Science Society of America Journal, v. 44, p. 892–898.

Wittwer, C.S., Bodvarsson, G.S., Chornack, M.P., Flint, A.L., Flint, L.E., Lewis, B.D., Spengler, R.W., and Rautman, C.A., 1992, Design of a three-dimensional site-scale model for the unsaturated zone at Yucca Mountain, Nevada: Proceedings International High-Level Radioactive Waste Conference, Las Vegas, Nevada, April 12–16, 1992, p. 263–271.

APPENDIX I: DATA OF PHYSICAL PROPERTIES AND FLOW PROPERTIES FOR EIGHT OUTCROP TRANSECTS

Table I-1. Solitario Canyon vertical transect physical properties, dry bulk density, porosity, and particle density calculated using relative-humidity oven and 105°C oven-dry weights; saturated hydraulic conductivity and sorptivity calculated from imbibition experiments on relative-humidity-dried samples. Estimates of saturated hydraulic conductivity done using regression equations in table 3.

Sample ID	Litho-logy	Tran-sect dis-tance (m)	Relative-humidity oven dried			105°C oven dried			Measured saturated hydraulic conduc-tivity (m/s)	Estimated saturated hydraulic conduc-tivity (m/s)	RH-dried sorp-tivity ($m/s^{0.5}$)
			Dry bulk density (g/cm^3)	Porosity (cm^3/cm^3)	Particle density (g/cm^3)	Dry bulk density (g/cm^3)	Porosity (cm^3/cm^3)	Particle density (g/cm^3)			
TPC60	cuc	0.0	1.84	0.272	2.53	1.84	0.274	2.54	4.8E-07		
TPC59	cuc	1.7	1.75	0.303	2.51	1.75	0.305	2.52		2.1E-07	
TPC58	cuc	1.7	1.80	0.279	2.50	1.80	0.282	2.51		9.3E-08	
TPC57	cuc	3.5	1.93	0.237	2.53	1.93	0.237	2.53	2.4E-07		9.7E-06
TPC56	cuc	5.3	2.14	0.149	2.52	2.14	0.149	2.52		2.5E-10	
TPC55-2	cuc	7.2	1.95	0.226	2.52	1.95	0.227	2.52	4.9E-08		
TPC54	cuc	9.3	2.12	0.156	2.51	2.12	0.157	2.52	8.7E-11		6.0E-05
TPC53	cul	11.4	2.21	0.116	2.50	2.21	0.117	2.50	3.4E-11		2.8E-06
TPC52	cul	13.1	2.18	0.116	2.47	2.18	0.116	2.47		3.6E-11	
TPC51	cul	14.5	2.21	0.106	2.47	2.21	0.107	2.48		2.0E-11	
TPC50	cul	16.3	2.22	0.096	2.46	2.22	0.098	2.46	1.7E-12		9.2E-07
TPC49	cul	18.9	2.29	0.053	2.41	2.28	0.059	2.42		6.3E-13	
TPC48	cul	18.9	2.26	0.067	2.42	2.26	0.068	2.43		1.7E-12	
TPC47	cul	21.9	2.21	0.104	2.46	2.21	0.105	2.47		1.8E-11	
TPC46-1	cul	25.8	2.19	0.108	2.46	2.19	0.109	2.46		2.2E-11	
TPC45	cul	26.4	2.19	0.105	2.45	2.19	0.107	2.46		1.9E-11	
TPC44	cks	29.7	2.10	0.160	2.50	2.10	0.160	2.50		4.4E-10	
TPC43	cks	30.8	2.21	0.103	2.46	2.20	0.104	2.46		1.7E-11	
TPC42	cks	32.3	2.23	0.093	2.45	2.22	0.096	2.46		9.3E-12	
TPC41	cks	34.3	2.23	0.093	2.46	2.23	0.095	2.46		9.1E-12	
TPC40	cks	36.4	2.27	0.052	2.40	2.27	0.054	2.40		6.0E-13	
TPC39	cks	41.3	2.23	0.095	2.47	2.23	0.097	2.47		1.0E-11	
TPC38	cks	43.1	2.24	0.094	2.47	2.24	0.096	2.48	3.6E-12		1.4E-06
TPC37	cks	44.8	2.28	0.066	2.44	2.27	0.071	2.44		1.5E-12	
TPC36	cks	47.4	2.30	0.035	2.38	2.29	0.041	2.39		1.9E-13	
TPC35	cks	49.5	2.24	0.093	2.47	2.24	0.096	2.47		8.9E-12	
TPC34	cks	54.4	2.32	0.061	2.47	2.31	0.064	2.47	2.7E-12		1.1E-06
TPC33	cks	56.5	2.24	0.093	2.47	2.23	0.096	2.47		9.1E-12	
TPC32	cks	59.6	2.29	0.070	2.47	2.29	0.076	2.47		2.1E-12	
TPC30	cks	64.2	2.29	0.066	2.45	2.29	0.068	2.45		1.6E-12	
TPC31	cks	64.2	2.30	0.062	2.46	2.30	0.063	2.46	2.8E-12		1.4E-06
TPC29	cll	65.1	2.14	0.140	2.48	2.14	0.140	2.48		1.4E-10	
TPC28	cll	67.5	2.30	0.074	2.49	2.30	0.076	2.49		2.7E-12	
TPC27	cll	69.5	2.17	0.118	2.46	2.17	0.119	2.47	1.3E-13		3.3E-06
TPC26	cll	72.5	2.01	0.188	2.48	2.01	0.189	2.48		1.8E-09	
TPC25	cll	75.4	2.22	0.105	2.48	2.22	0.108	2.49		1.9E-11	
TPC24	cll	78.5	2.34	0.061	2.49	2.34	0.063	2.50		1.1E-12	
TPC23	cll	81.2	2.30	0.077	2.49	2.30	0.077	2.49		3.3E-12	
TPC22-3	cll	84.6	2.33	0.064	2.49	2.33	0.065	2.50	2.0E-09		3.4E-06
TPC21	cll	85.5	2.30	0.073	2.48	2.30	0.075	2.49		2.5E-12	
TPC20	cll	88.1	2.28	0.076	2.47	2.28	0.078	2.47		3.0E-12	
TPC18	cll	89.3	2.31	0.063	2.47	2.31	0.065	2.47		1.3E-12	
TPC19	cll	89.3	2.28	0.080	2.48	2.28	0.081	2.48		4.0E-12	
TPC17	cll	91.0	2.37	0.042	2.48	2.37	0.045	2.48		2.9E-13	

Table I-1. Solitario Canyon vertical transect physical properties, dry bulk density, porosity, and particle density calculated using relative-humidity oven and 105°C oven-dry weights; saturated hydraulic conductivity and sorptivity calculated from imbibition experiments on relative-humidity-dried samples. Estimates of saturated hydraulic conductivity done using regression equations in table 3.--Continued

Sample ID	Lithology	Transect distance (m)	Relative-humidity oven dried: Dry bulk density (g/cm^3)	Relative-humidity oven dried: Porosity (cm^3/cm^3)	Relative-humidity oven dried: Particle density (g/cm^3)	105°C oven dried: Dry bulk density (g/cm^3)	105°C oven dried: Porosity (cm^3/cm^3)	105°C oven dried: Particle density (g/cm^3)	Measured saturated hydraulic conductivity (m/s)	Estimated saturated hydraulic conductivity (m/s)	RH-dried sorptivity ($m/s^{0.5}$)
TPC16	cll	93.4	2.34	0.057	2.49	2.34	0.059	2.49	3.8E-12		2.8E-06
TPC15-2	cll	95.9	2.33	0.068	2.50	2.33	0.070	2.51		1.8E-12	
TPC13	ch	99.2	2.30	0.071	2.48	2.30	0.073	2.48		2.2E-12	
TPC14-2	ch	99.2	2.32	0.072	2.50	2.32	0.072	2.50		2.3E-12	
TPC12	ch	101.5	2.35	0.053	2.48	2.35	0.055	2.48	3.6E-12		1.2E-06
TPC11	ch	104.1	2.35	0.044	2.46	2.35	0.047	2.47		3.4E-13	
TPC10	ch	105.8	2.35	0.049	2.48	2.35	0.052	2.48		4.9E-13	
TPC9	ch	106.7	2.36	0.038	2.45	2.35	0.042	2.46		2.3E-13	
TPC8	cc	109.6	2.38	0.039	2.48	2.37	0.043	2.48	3.7E-13		7.1E-07
TPC7	cc	111.6	2.37	0.049	2.50	2.37	0.052	2.50		4.8E-13	
TPC6	cc	113.5	2.37	0.040	2.47	2.37	0.043	2.48		2.6E-13	
TPC5	cc	116.3	2.33	0.022	2.39	2.33	0.026	2.39	1.2E-08		5.4E-06
TPC4	cc	117.8	2.30	0.024	2.36	2.29	0.030	2.36	1.5E-09		
TPC3	cc	120.2	2.33	0.021	2.38	2.33	0.027	2.39		6.7E-14	
TPC2	cv	123.7	2.31	0.030	2.38	2.31	0.031	2.38	4.5E-10		1.1E-06
TPC1	cv	125.7	2.09	0.110	2.34	2.08	0.111	2.34		2.5E-11	
BT27-1V	ccb	126.2	1.93	0.172	2.33	1.86	0.232	2.42		8.5E-10	
BT27H	ccb	126.2	1.98	0.155	2.34	1.94	0.181	2.37	4.2E-09		6.6E-06
BT26H	ccb	127.1	1.95	0.176	2.37	1.91	0.203	2.40		1.0E-09	
BT25H	ccb	128.6	1.57	0.312	2.28	1.54	0.331	2.30	5.8E-08		3.1E-05
BT25-2V	ccb	128.6	1.55	0.317	2.27	1.52	0.346	2.32		3.4E-07	
BT25-1V	ccb	128.6	1.59	0.296	2.26	1.55	0.328	2.31		1.7E-07	
BT24V	ccb	129.8	1.40	0.391	2.30	1.37	0.409	2.32		2.3E-06	
BT24H	ccb	129.8	1.40	0.388	2.29	1.37	0.407	2.32	2.0E-06		1.7E-04
BT23H	ccb	130.5	1.35	0.407	2.29	1.31	0.444	2.36	5.4E-06		2.7E-04
BT23-1H	ccb	130.5	1.39	0.392	2.29	1.35	0.419	2.33	3.6E-06		2.3E-04
BT23V	ccb	130.5	1.34	0.415	2.29	1.32	0.429	2.31		3.6E-06	
BT22V	ccb	131.5	1.36	0.407	2.30	1.33	0.435	2.35		3.2E-06	
BT22H	ccb	131.5	1.40	0.389	2.30	1.37	0.417	2.35	1.6E-06		7.0E-05
BT21V	ccb	132.3	1.36	0.411	2.31	1.32	0.448	2.39	4.4E-06		9.1E-05
BT21H	ccb	132.3	1.28	0.447	2.32	1.26	0.462	2.34		5.8E-06	
BT20H	ccb	133.5	0.97	0.582	2.32	0.93	0.617	2.42	5.5E-05		5.8E-04
BT20V	ccb	133.5	0.93	0.599	2.33	0.91	0.620	2.39		7.8E-06	
BT19H	ym	133.8	1.27	0.450	2.31	1.24	0.473	2.35		6.0E-06	
BT18H	ym	134.3	1.34	0.412	2.28	1.30	0.440	2.32	1.3E-06		2.5E-04
BT17	ym	134.9	1.34	0.413	2.29	1.31	0.442	2.34	3.1E-06		9.3E-05
BT16V	ym	135.6	1.34	0.431	2.35	1.30	0.461	2.40		4.7E-06	
BT16H	ym	135.6	1.26	0.440	2.26	1.24	0.463	2.30		5.3E-06	
BT15	ym	136.1	1.49	0.375	2.38	1.44	0.399	2.40		1.6E-06	
BT14H	pc	137.5	1.33	0.441	2.39	1.30	0.468	2.44		5.4E-06	
BT14V	pc	137.5	1.32	0.444	2.38	1.29	0.463	2.41	2.0E-05		3.4E-04
BT11V	pc	139.9	1.13	0.520	2.35	1.10	0.535	2.37		1.0E-05	
BT11	pc	139.9	0.98	0.569	2.28	0.98	0.571	2.27	3.4E-06		4.5E-04
BT32	bt	141.1	1.00	0.588	2.41	0.98	0.596	2.43		8.5E-06	

Table I-1. Solitario Canyon vertical transect physical properties, dry bulk density, porosity, and particle density calculated using relative-humidity oven and 105°C oven-dry weights; saturated hydraulic conductivity and sorptivity calculated from imbibition experiments on relative-humidity-dried samples. Estimates of saturated hydraulic conductivity done using regression equations in table 3.--Continued

Sample ID	Litho-logy	Tran-sect dis-tance (m)	Relative-humidity oven dried			105°C oven dried			Measured saturated hydraulic conduc-tivity (m/s)	Estimated saturated hydraulic conduc-tivity (m/s)	RH-dried sorp-tivity ($m/s^{0.5}$)
			Dry bulk density (g/cm^3)	Porosity (cm^3/cm^3)	Particle density (g/cm^3)	Dry bulk density (g/cm^3)	Porosity (cm^3/cm^3)	Particle density (g/cm^3)			
BT10	bt	141.1	1.10	0.563	2.52	1.06	0.591	2.60		9.8E-06	
BT31	bt	141.3	0.92	0.618	2.42	0.90	0.635	2.47		6.4E-06	
BT30V	bt	142.2	0.99	0.581	2.36	0.97	0.590	2.38		8.9E-06	
BT30V	bt	142.2	1.03	0.562	2.35	1.01	0.571	2.36		9.8E-06	
BT29H	bt	143.0	0.98	0.595	2.42	0.97	0.603	2.43		8.1E-06	
BT28	bt	143.6	0.91	0.617	2.37	0.89	0.623	2.36		6.5E-06	
BT9H	bt	143.9	1.02	0.574	2.40	0.99	0.601	2.48		9.3E-06	
BT9V	bt	143.9	1.07	0.549	2.37	1.04	0.572	2.44	3.3E-06		1.2E-04
BT8H	bt	144.5	1.15	0.525	2.42	1.13	0.540	2.46		1.0E-05	
BT8V	bt	144.5	1.04	0.569	2.42	1.02	0.582	2.45		9.5E-06	
BT7-2H	bt	146.0	1.11	0.544	2.43	1.09	0.556	2.46		1.0E-05	
BT7V	bt	146.0	1.09	0.552	2.44	1.08	0.565	2.47		1.0E-05	
BT6	bt	146.8	1.67	0.349	2.56	1.65	0.355	2.57		8.4E-07	
BT5V	bt	147.5	1.53	0.383	2.48	1.51	0.392	2.48		1.9E-06	
BT4V	bt	148.4	1.45	0.413	2.48	1.44	0.418	2.48		3.5E-06	
BT4H	bt	148.4	1.53	0.387	2.50	1.52	0.390	2.49		2.1E-06	
BT3H	bt	148.7	1.61	0.369	2.55	1.60	0.370	2.54		1.4E-06	
BT3-3V	bt	148.7	1.54	0.394	2.55	1.54	0.395	2.54	5.0E-07		8.3E-05
BT1	tc,vitric	149.0	2.48	0.039	2.58	2.44	0.044	2.56		2.5E-13	
BT2	tc,vitric	149.0	2.45	0.054	2.59	2.41	0.058	2.55		7.1E-13	
TS59-1	tc	149.7	2.39	0.017	2.43	2.37	0.020	2.42		5.2E-14	
TS59-2	tc	149.7	2.37	0.024	2.43	2.36	0.026	2.42		8.5E-14	
TS58	tc	151.5	2.28	0.118	2.58	2.26	0.121	2.57	1.3E-09		1.5E-05
TS57	tr	153.6	2.22	0.134	2.57	2.21	0.138	2.56		1.1E-10	
TS56	tr	155.6	2.20	0.148	2.58	2.18	0.152	2.57	4.2E-07		2.2E-05
TS55	tr	158.2	2.24	0.125	2.56	2.22	0.128	2.55		6.2E-11	
TS54	tr	160.5	2.17	0.149	2.55	2.16	0.151	2.54	2.7E-09		1.9E-05
TS53	tr	162.3	2.16	0.155	2.56	2.13	0.157	2.52		3.4E-10	
TS52	tr	163.4	2.20	0.143	2.57	2.18	0.144	2.55	4.7E-09		
TS51	tr	165.8	2.22	0.131	2.56	2.21	0.131	2.54		8.8E-11	
TS50	tr	167.9	2.18	0.145	2.55	2.17	0.147	2.55	5.5E-09		1.9E-05
TS49	tr	170.5	2.27	0.109	2.54	2.25	0.112	2.54		2.4E-11	
TS48	tr	173.1	2.17	0.150	2.55	2.15	0.152	2.54		2.6E-10	
TS46	tul	176.3	2.04	0.192	2.52	2.02	0.195	2.51		2.3E-09	
TS45	tul	182.7	2.14	0.151	2.52	2.13	0.155	2.51		2.7E-10	
TS44	tul	183.8	2.16	0.140	2.52	2.15	0.142	2.50		1.5E-10	
TS43	tul	186.5	1.96	0.214	2.49	1.94	0.216	2.47		6.6E-09	
TS42	tul	188.7	2.19	0.133	2.53	2.17	0.136	2.51		9.7E-11	
TS41	tul	192.6	2.04	0.188	2.51	2.01	0.191	2.49		1.9E-09	
TS40	tul	194.5	2.11	0.156	2.50	2.10	0.159	2.49	5.5E-10		7.8E-06
TS39	tul	196.9	2.17	0.124	2.48	2.16	0.128	2.48		5.9E-11	
TS38	tul	198.7	2.13	0.145	2.49	2.12	0.147	2.48		1.9E-10	
TS37	tul	200.9	2.08	0.164	2.49	2.06	0.169	2.48		5.4E-10	
TS36	tul	203.3	2.13	0.146	2.50	2.12	0.150	2.49		2.1E-10	

Table I-1. Solitario Canyon vertical transect physical properties, dry bulk density, porosity, and particle density calculated using relative-humidity oven and 105°C oven-dry weights; saturated hydraulic conductivity and sorptivity calculated from imbibition experiments on relative-humidity-dried samples. Estimates of saturated hydraulic conductivity done using regression equations in table 3.--Continued

Sample ID	Litho-logy	Tran-sect dis-tance (m)	Relative-humidity oven dried			105°C oven dried			Measured saturated hydraulic conduc-tivity (m/s)	Estimated saturated hydraulic conduc-tivity (m/s)	RH-dried sorp-tivity ($m/s^{0.5}$)
			Dry bulk density (g/cm^3)	Porosity (cm^3/cm^3)	Particle density (g/cm^3)	Dry bulk density (g/cm^3)	Porosity (cm^3/cm^3)	Particle density (g/cm^3)			
TS35	tul	205.9	2.11	0.152	2.48	2.09	0.156	2.48		2.9E-10	
TS34	tul	207.9	2.15	0.162	2.57	2.14	0.165	2.56		4.8E-10	
TS33	tul	210.8	2.09	0.156	2.48	2.07	0.160	2.47		3.5E-10	
TS32	tul	212.4	2.19	0.120	2.49	2.18	0.124	2.49	4.1E-12		2.6E-06
TS31	tul	215.2	2.17	0.129	2.49	2.14	0.133	2.47		8.0E-11	
TS30	tul	215.2	2.23	0.104	2.49	2.21	0.108	2.48		1.8E-11	
TS29	tul	217.9	2.24	0.099	2.49	2.23	0.103	2.48	5.5E-13		3.7E-06
TS28	tul	219.5	2.24	0.100	2.49	2.22	0.104	2.48		1.4E-11	
TS27	tul	221.1	2.28	0.085	2.49	2.26	0.089	2.48		5.6E-12	
TS26	tul	223.1	2.17	0.129	2.49	2.16	0.131	2.48	3.2E-11		3.6E-06
TS26-2	tul	223.1	2.18	0.124	2.49	2.17	0.126	2.48		6.0E-11	
TS25	tul	225.9	2.21	0.113	2.49	2.19	0.115	2.47		3.1E-11	
TS24	tul	228.0	2.08	0.167	2.50	2.06	0.170	2.48		6.5E-10	
TS23	tul	229.8	2.26	0.082	2.46	2.23	0.092	2.45		4.5E-12	
TS22	tul	232.4	2.32	0.065	2.48	2.29	0.069	2.46		1.5E-12	
TS21-2	tul	235.0	2.31	0.077	2.50	2.26	0.083	2.47		3.3E-12	
TS21-1	tul	235.0	2.26	0.096	2.50	2.22	0.100	2.47		1.1E-11	
TS20	tul	237.1	2.32	0.066	2.48	2.29	0.072	2.47		1.6E-12	
TS19	tul	239.9	2.36	0.058	2.50	2.31	0.063	2.47		8.9E-13	
TS18	tul	242.9	2.34	0.058	2.48	2.31	0.064	2.46		9.2E-13	
TS17	tul	245.7	2.35	0.064	2.51	2.32	0.068	2.50		1.4E-12	
TS16	tmn	246.7	2.21	0.105	2.47	2.20	0.107	2.46		1.8E-11	
TS15	tmn	249.2	2.21	0.109	2.48	2.20	0.110	2.47		2.4E-11	
TS14	tmn	252.4	2.22	0.095	2.46	2.21	0.101	2.45		1.0E-11	
TS13	tmn	255.1	2.22	0.102	2.48	2.21	0.107	2.47		1.5E-11	
TS12	tmn	257.9	2.28	0.095	2.52	2.26	0.099	2.51		1.0E-11	
TS11	tmn	263.3	2.31	0.070	2.49	2.28	0.073	2.46		2.0E-12	
TS10	tll	265.9	2.36	0.049	2.48	2.33	0.055	2.47		5.0E-13	
TS9	tll	267.9	2.36	0.059	2.50	2.34	0.064	2.50		9.5E-13	
TS8	tll	275.2	2.35	0.075	2.54	2.32	0.077	2.51		2.8E-12	
TS7	tll	281.5	2.35	0.089	2.58	2.32	0.092	2.56	6.8E-12		
TS6	tll	285.6	2.34	0.092	2.58	2.31	0.096	2.56	8.2E-12		
TS5	tll	289.9	2.36	0.078	2.56	2.34	0.083	2.55	3.4E-12		
TS4	tll	293.8	2.32	0.063	2.48	2.30	0.072	2.48	1.3E-12		
TS3	tll	301.4	2.34	0.066	2.50	2.32	0.070	2.50	1.6E-12		
TS2	tll	303.7	2.35	0.062	2.50	2.33	0.067	2.50	1.2E-12		
TS1	tll	314.6	2.29	0.035	2.37	2.24	0.064	2.39	1.8E-13		

Table I-2. Busted Butte vertical transect physical properties, dry bulk density, porosity, and particle density calculated using relative-humidity oven and 105°C oven-dry weights; saturated hydraulic conductivity and sorptivity calculated from imbibition experiments on relative-humidity-dried samples

Sample ID	Lithology	Transect distance (m)	Relative-humidity oven dried			105°C oven dried			Saturated hydraulic conductivity (m/s)
			Dry bulk density (g/cm^3)	Porosity (cm^3/cm^3)	Particle density (g/cm^3)	Dry bulk density (g/cm^3)	Porosity (cm^3/cm^3)	Particle density (g/cm^3)	
BB101	tn	173.4	1.98	0.174	2.40	1.96	0.196	2.43	4.2E-10
BB100	tn	172.8	1.67	0.304	2.40	1.66	0.309	2.40	6.5E-09
BB102	tc, vitric	171.9	2.36	0.045	2.47	2.35	0.049	2.47	1.7E-09
BB99	tc, vitric	171.9	2.32	0.042	2.42	2.32	0.045	2.43	
BB98	tc, vitric	171.0	2.30	0.046	2.41	2.29	0.049	2.41	2.6E-10
BB97	tc	169.5	2.16	0.132	2.48	2.15	0.136	2.49	
BB96	tc	167.9	2.16	0.135	2.50	2.15	0.142	2.51	2.9E-08
BB95	tr	166.1	2.11	0.139	2.46	2.11	0.140	2.46	8.2E-10
BB94	tr	164.9	2.02	0.170	2.43	2.02	0.170	2.43	1.6E-10
BB93	tr	162.8	2.18	0.123	2.49	2.18	0.124	2.49	
BB92	tr	160.3	2.14	0.118	2.42	2.14	0.119	2.42	
BB91	tr	158.5	2.02	0.181	2.47	2.02	0.181	2.47	
BB90	tul	154.8	2.22	0.092	2.44	2.21	0.096	2.45	
BB89	tul	153.0	2.12	0.131	2.44	2.12	0.135	2.45	5.4E-12
BB88	tul	151.5	2.19	0.098	2.43	2.19	0.104	2.44	
BB87	tul	150.0	2.10	0.151	2.47	2.09	0.155	2.48	
BB86	tul	148.4	2.26	0.077	2.44	2.25	0.084	2.45	1.8E-12
BB85	tul	146.3	2.25	0.080	2.44	2.24	0.084	2.45	
BB84	tul	144.8	2.09	0.151	2.46	2.08	0.161	2.48	
BB83	tul	141.1	2.22	0.096	2.46	2.21	0.101	2.46	
BB82	tul	139.0	2.24	0.095	2.48	2.24	0.099	2.49	
BB81	tul	137.5	2.20	0.105	2.46	2.20	0.111	2.47	
BB80	tul	133.2	2.38	0.050	2.50	2.38	0.053	2.51	
BB79	tul	131.4	2.22	0.106	2.48	2.22	0.111	2.49	
BB78	tul	130.1	2.13	0.144	2.49	2.12	0.152	2.50	
BB77	tul	129.2	2.15	0.140	2.50	2.14	0.147	2.51	
BB76	tul	126.8	2.16	0.130	2.48	2.15	0.137	2.50	
BB75	tul	125.9	2.29	0.068	2.46	2.29	0.076	2.47	
BB74	tul	124.4	2.33	0.076	2.52	2.32	0.085	2.54	
BB73	tul	122.5	2.25	0.104	2.51	2.25	0.107	2.52	
BB72	tul	121.3	2.29	0.086	2.51	2.29	0.090	2.51	
BB71	tul	119.2	2.33	0.065	2.49	2.32	0.070	2.50	
BB70	tul	116.7	2.34	0.057	2.48	2.33	0.064	2.49	3.2E-12
BB69	tul	99.4	2.34	0.063	2.49	2.33	0.067	2.50	
BB68	tmn	96.3	2.34	0.063	2.49	2.33	0.070	2.50	
BB67	tmn	95.1	2.30	0.085	2.51	2.29	0.091	2.52	
BB66	tmn	90.2	2.23	0.078	2.42	2.23	0.083	2.43	
BB65	tmn	86.9	2.02	0.172	2.44	2.02	0.175	2.45	
BB64	tmn	84.4	2.05	0.177	2.49	2.04	0.180	2.49	
BB63	tmn	81.4	2.24	0.064	2.39	2.23	0.073	2.40	
BB60	tll	71.0	2.25	0.067	2.42	2.25	0.072	2.42	
BB59	tll	68.6	2.36	0.051	2.49	2.35	0.060	2.50	

Table I-2. Busted Butte vertical transect physical properties, dry bulk density, porosity, and particle density calculated using relative-humidity oven and 105°C oven-dry weights; saturated hydraulic conductivity and sorptivity calculated from imbibition experiments on relative-humidity-dried samples--Continued

Sample ID	Lithology	Transect distance (m)	Relative-humidity oven dried			105°C oven dried			Saturated hydraulic conductivity (m/s)
			Dry bulk density (g/cm³)	Porosity (cm³/cm³)	Particle density (g/cm³)	Dry bulk density (g/cm³)	Porosity (cm³/cm³)	Particle density (g/cm³)	
BB58	tll	66.4	2.30	0.072	2.48	2.30	0.076	2.49	
BB57	tll	64.9	2.35	0.068	2.52	2.34	0.073	2.53	
BB56	tll	62.8	2.34	0.066	2.50	2.33	0.073	2.51	
BB55	tll	60.7	2.33	0.060	2.47	2.32	0.064	2.48	
BB54	tll	59.7	2.26	0.090	2.49	2.26	0.095	2.49	4.0E-13
BB53	tll	57.0	2.32	0.061	2.47	2.31	0.067	2.48	
BB52	tll	55.5	2.34	0.023	2.40	2.34	0.029	2.41	
BB51	tll	53.6	2.32	0.059	2.47	2.32	0.066	2.48	
BB50	tll	50.6	2.33	0.065	2.49	2.33	0.072	2.51	
BB49	tll	48.2	2.35	0.077	2.55	2.35	0.078	2.55	
BB48	tll	46.3	2.07	0.170	2.50	2.07	0.173	2.50	
BB47	tll	44.8	2.33	0.078	2.53	2.32	0.086	2.54	
BB46	tll	42.7	2.32	0.064	2.48	2.32	0.069	2.49	
BB45	tll	40.5	2.18	0.123	2.48	2.17	0.129	2.50	
BB44	tll	38.7	2.35	0.057	2.49	2.34	0.067	2.51	
BB43	tll	37.5	2.32	0.064	2.47	2.30	0.075	2.49	
BB42	tll	36.6	2.32	0.062	2.48	2.32	0.069	2.49	
BB41C	tll	35.4	2.33	0.057	2.47	2.32	0.068	2.49	
BB40	tll	34.4	2.28	0.054	2.41	2.28	0.058	2.42	
BB39	tll	33.5	2.28	0.078	2.48	2.27	0.088	2.49	
BB38	tll	32.6	1.99	0.203	2.50	1.99	0.204	2.50	
BB37	tll	32.0	2.20	0.116	2.49	2.19	0.127	2.50	1.2E-10
BB36	tll	31.1	2.32	0.074	2.50	2.31	0.083	2.52	
BB35	tll	31.1	2.32	0.068	2.49	2.32	0.073	2.50	
BB34	tll	30.2	2.28	0.102	2.54	2.27	0.110	2.55	
BB33	tll	29.3	2.32	0.068	2.49	2.31	0.075	2.50	4.5E-13
BB32	tll	28.0	2.33	0.084	2.55	2.33	0.088	2.55	
BB31	tll	26.8	2.35	0.091	2.59	2.35	0.095	2.59	
BB30	tll	25.3	2.36	0.080	2.57	2.36	0.086	2.58	
BB29	tll	24.4	2.34	0.073	2.52	2.33	0.083	2.54	
BB28	tll	23.2	1.98	0.207	2.50	1.98	0.207	2.50	
BB27	tll	22.6	2.30	0.061	2.45	2.29	0.069	2.46	
BB26	tll	21.6	2.34	0.076	2.53	2.33	0.083	2.54	
BB25	tll	21.0	2.08	0.167	2.49	2.08	0.168	2.50	
BB24	tm	20.1	2.34	0.091	2.57	2.34	0.096	2.58	
BB23	tm	19.5	2.34	0.088	2.57	2.34	0.091	2.57	
BB22A	tm	18.6	2.34	0.068	2.51	2.34	0.074	2.52	
BB22	tm	18.6	2.34	0.067	2.51	2.33	0.078	2.53	
BB21	tm	18.0	2.31	0.068	2.47	2.30	0.073	2.48	
BB20	tm	17.4	2.35	0.066	2.52	2.35	0.070	2.52	
BB19	tm	16.5	2.19	0.132	2.52	2.19	0.133	2.52	
BB18	tm	15.8	2.36	0.086	2.59	2.36	0.090	2.59	

Table I-2. Busted Butte vertical transect physical properties, dry bulk density, porosity, and particle density calculated using relative-humidity oven and 105°C oven-dry weights; saturated hydraulic conductivity and sorptivity calculated from imbibition experiments on relative-humidity-dried samples--Continued

Sample ID	Lithology	Transect distance (m)	Relative-humidity oven dried			105°C oven dried			Saturated hydraulic conductivity (m/s)
			Dry bulk density (g/cm^3)	Porosity (cm^3/cm^3)	Particle density (g/cm^3)	Dry bulk density (g/cm^3)	Porosity (cm^3/cm^3)	Particle density (g/cm^3)	
BB17	tm	15.5	2.38	0.074	2.58	2.38	0.077	2.58	
BB16	tm	14.6	2.37	0.073	2.55	2.36	0.074	2.55	
BB15	tm	13.7	2.37	0.069	2.55	2.37	0.074	2.55	
BB14	tm	12.8	2.31	0.101	2.57	2.30	0.103	2.57	
BB13A	tm	12.2	2.34	0.092	2.58	2.34	0.096	2.59	
BB13	tm	12.2	2.34	0.063	2.50	2.34	0.063	2.50	
BB12	tm	11.6	2.33	0.096	2.58	2.33	0.096	2.58	
BB11	tm	11.0	2.21	0.101	2.46	2.21	0.104	2.47	
BB10	tm	10.4	2.39	0.078	2.59	2.38	0.080	2.59	
BB9	tv	9.4	2.34	0.017	2.38	2.33	0.024	2.39	
BB8	tv	9.1	2.35	0.012	2.38	2.35	0.019	2.39	
BB7	tv	6.1	2.35	0.012	2.37	2.34	0.018	2.38	
BB6	tv	4.6	2.35	0.010	2.37	2.34	0.017	2.38	
BB5	tv	3.4	2.34	0.014	2.37	2.34	0.020	2.38	
BB4	tv	1.8	2.28	0.014	2.31	2.27	0.021	2.32	
BB3	tv	0.9	2.36	0.010	2.38	2.35	0.016	2.39	
BB2	tv	0.0	2.30	0.012	2.33	2.30	0.017	2.34	
BB1	tv	0.0	2.35	0.014	2.38	2.34	0.017	2.38	

Table I-3. Yucca Wash vertical transect physical properties, dry bulk density, porosity, and particle density calculated using relative-humidity oven and 105°C oven-dry weights; saturated hydraulic conductivity and sorptivity calculated from imbibition experiments. Estimates of saturated hydraulic conductivity done using regression equations in table 3.

Sample ID	Litho-logy	Transect distance (m)	Relative-humidity oven dried			105°C oven dried			Measured saturated hydraulic conduc-tivity (m/s)	Estimated saturated hydraulic conductivity (m/s)
			Dry bulk density (g/cm³)	Porosity (cm³/cm³)	Particle density (g/cm³)	Dry bulk density (g/cm³)	Porosity (cm³/cm³)	Particle density (g/cm³)		
UPR-117	ccr	0.0	2.13	0.174	2.57	2.12	0.183	2.59	4.2E-09	
UPR-116	ccr	1.4	2.13	0.171	2.57	2.13	0.175	2.58	7.6E-10	
UPR-115	ccr	2.6	2.04	0.190	2.52	2.04	0.195	2.53	2.7E-09	
UPR-114	ccr	3.5	2.23	0.115	2.52	2.22	0.124	2.54	4.2E-09	
UPR-113	ccr	3.7	2.18	0.156	2.58	2.15	0.185	2.64	6.0E-09	
UPR-112	ccr	4.1	1.89	0.278	2.61	1.88	0.282	2.62	6.7E-08	
UPR-111	ccr	4.4	1.89	0.278	2.62	1.89	0.279	2.63	1.8E-08	
UPR-110	ccr	6.6	1.73	0.309	2.50	1.73	0.312	2.51	7.1E-10	
UPR-109	ccr	8.2	1.70	0.337	2.56	1.69	0.342	2.57	2.2E-07	
UPR-108	ccr	10.5	1.86	0.280	2.58	1.86	0.284	2.59	1.1E-08	
UPR-107	ccr	11.7	1.91	0.271	2.62	1.91	0.273	2.62	1.1E-08	
UPR-106	ccr	13.1	1.82	0.302	2.60	1.81	0.304	2.61	3.7E-08	
UPR-105	ccr	15.2	1.91	0.271	2.62	1.91	0.273	2.62	3.1E-08	
UPR-104	cl	20.7	2.35	0.075	2.54	2.34	0.080	2.55		2.5E-11
UPR-103	cl	22.9	2.35	0.076	2.54	2.34	0.081	2.55		2.6E-11
UPR-102	cc	25.3	2.30	0.051	2.42	2.28	0.069	2.45		9.8E-12
UPR-101	cc	27.4	2.21	0.043	2.30	2.19	0.053	2.32		7.1E-12
UPR-100	cc	30.8	2.08	0.150	2.45	2.08	0.152	2.45	6.8E-10	
UPR-99	cc	32.5	2.10	0.139	2.44	2.10	0.146	2.45	1.2E-10	
UPR-98	cc	33.5	2.18	0.125	2.49	2.17	0.128	2.49	2.7E-10	
UPR-97	cc	35.1	2.21	0.115	2.50	2.21	0.117	2.50	1.3E-10	
UPR-96	cc	36.6	2.25	0.101	2.50	2.24	0.105	2.51		6.6E-11
UPR-95	cc	38.3	2.13	0.125	2.43	2.13	0.128	2.44	5.2E-10	
UPR-94	cc	39.3	2.16	0.137	2.50	2.15	0.141	2.50	5.1E-10	
UPR-93	ccb	40.7	1.68	0.322	2.48	1.67	0.329	2.49	2.4E-07	
UPR-92	ccb	42.2	1.41	0.435	2.50	1.41	0.439	2.51	8.4E-07	
UPR-91	ccb	43.7	1.35	0.459	2.50	1.34	0.469	2.53	6.4E-07	
UPR-90	ccb	44.7	1.37	0.456	2.51	1.36	0.462	2.53	3.8E-07	
UPR-89	ccb	46.2	1.22	0.496	2.42	1.21	0.505	2.45	9.2E-07	
UPR-88	ccb	46.9	1.22	0.512	2.49	1.20	0.526	2.54	1.4E-06	
UPR-87	ccb	48.2	1.26	0.489	2.48	1.26	0.497	2.50	5.5E-07	
UPR-86	ccb	50.7	1.28	0.426	2.23	1.21	0.494	2.40	2.8E-08	
UPR-85	ccb	51.8	1.27	0.445	2.28	1.25	0.461	2.32	5.8E-06	
UPR-84	ccb	53.9	1.33	0.419	2.30	1.31	0.440	2.35	3.7E-06	
UPR-83	ccb	55.5	1.15	0.496	2.29	1.13	0.518	2.34	1.1E-05	
UPR-82	ccb	56.1	1.24	0.462	2.30	1.22	0.486	2.37	1.7E-05	
UPR-81	bt	56.7	1.03	0.545	2.27	1.01	0.573	2.36	1.1E-05	
UPR-80	bt	57.3	1.34	0.436	2.37	1.28	0.491	2.51	6.6E-07	
UPR-79	bt	57.6	0.93	0.592	2.28	0.84	0.684	2.65	9.9E-07	
UPR-78A	bt	58.5	0.88	0.616	2.29	0.83	0.664	2.47	3.3E-04	
UPR-78B	bt	58.5	0.88	0.611	2.27	0.83	0.654	2.40	3.3E-04	

Table I-3. Yucca Wash vertical transect physical properties, dry bulk density, porosity, and particle density calculated using relative-humidity oven and 105°C oven-dry weights; saturated hydraulic conductivity and sorptivity calculated from imbibition experiments. Estimates of saturated hydraulic conductivity done using regression equations in table 3.--Continued

Sample ID	Litho-logy	Transect distance (m)	Relative-humidity oven dried			105°C oven dried			Measured saturated hydraulic conduc-tivity (m/s)	Estimated saturated hydraulic conductivity (m/s)
			Dry bulk density (g/cm^3)	Porosity (cm^3/cm^3)	Particle density (g/cm^3)	Dry bulk density (g/cm^3)	Porosity (cm^3/cm^3)	Particle density (g/cm^3)		
UPR-77	bt	59.3	0.86	0.611	2.20	0.83	0.642	2.31	1.4E-04	
UPR-76	ymn	60.2	1.14	0.483	2.21	1.13	0.501	2.26	1.1E-05	
UPR-75	ymnl	61.1	1.31	0.410	2.22	1.30	0.422	2.25	1.8E-06	
UPR-74	ymnl	62.6	1.45	0.314	2.12	1.44	0.338	2.18	4.0E-07	
UPR-73	ymnl	62.6	1.45	0.326	2.15	1.44	0.326	2.13	4.0E-07	
UPR-72	ymnl	63.6	1.73	0.217	2.21	1.72	0.223	2.22	7.0E-09	
UPR-71	ymnl	65.2	1.77	0.283	2.47	1.77	0.287	2.48	4.9E-08	
UPR-70	ymnl	66.3	1.88	0.235	2.45	1.88	0.236	2.46	1.9E-08	
UPR-69	ymnl	67.5	1.98	0.185	2.43	1.98	0.188	2.44	6.8E-09	
UPR-68	ymnl	69.6	2.08	0.166	2.49	2.07	0.169	2.49	2.3E-09	
UPR-67	ymnl	71.0	2.20	0.106	2.46	2.19	0.119	2.48		7.8E-11
UPR-66	ymnl	73.0	2.23	0.079	2.42	2.22	0.086	2.43		2.9E-11
UPR-65	ymnl	76.4	2.31	0.052	2.43	2.30	0.055	2.44		1.0E-11
UPR-64	yml	80.3	2.33	0.061	2.48	2.32	0.066	2.49		1.5E-11
UPR-63	yml	83.4	2.28	0.072	2.46	2.28	0.071	2.46		2.2E-11
UPR-62	yml	83.4	2.34	0.057	2.48	2.33	0.064	2.49		1.3E-11
UPR-61	yml	84.3	2.31	0.068	2.48	2.31	0.071	2.48		1.9E-11
UPR-60	yml	85.5	2.34	0.057	2.48	2.33	0.063	2.49		1.3E-11
UPR-59	yml	87.3	2.30	0.078	2.49	2.30	0.081	2.50		2.8E-11
UPR-58	yml	89.0	2.30	0.072	2.48	2.29	0.076	2.48		2.2E-11
UPR-57	yml	91.0	2.31	0.072	2.49	2.31	0.075	2.50		2.2E-11
UPR-56	yml	92.5	2.31	0.065	2.47	2.30	0.072	2.48		1.7E-11
UPR-55	yml	93.7	2.31	0.071	2.49	2.30	0.079	2.50		2.1E-11
UPR-54	yml	95.1	2.28	0.069	2.45	2.27	0.074	2.46		2.0E-11
UPR-53	ymw	96.0	2.33	0.062	2.48	2.32	0.066	2.49		1.5E-11
UPR-52	ymw	98.3	2.33	0.053	2.46	2.33	0.058	2.47		1.1E-11
UPR-51	ymw	99.2	2.34	0.054	2.48	2.33	0.064	2.49		1.1E-11
UPR-50	ymw	100.7	2.34	0.055	2.47	2.33	0.059	2.48		1.2E-11
UPR-49	ymn	103.0	1.83	0.165	2.20	1.78	0.216	2.28		6.3E-10
UPR-48	ymn	104.7	1.40	0.374	2.24	1.37	0.402	2.30	3.6E-07	
UPR-47	ymn	105.6	1.38	0.401	2.30	1.29	0.491	2.53	2.6E-06	
UPR-46	bt	106.1	1.57	0.331	2.35	1.53	0.371	2.43	6.4E-06	
UPR-45	bt	107.0	1.41	0.393	2.32	1.38	0.424	2.39	2.4E-07	
UPR-44	bt	107.7	1.13	0.510	2.31	1.11	0.528	2.36	3.9E-06	
UPR-43	bt	108.7	1.48	0.360	2.31	1.44	0.398	2.39	2.4E-06	
UPR-42	bt	109.3	1.42	0.376	2.28	1.41	0.395	2.32	1.1E-06	
UPR-41	bt	109.7	1.35	0.413	2.30	1.33	0.435	2.36	1.1E-06	
UPR-40	rz	121.5	1.38	0.401	2.31	1.37	0.412	2.34	1.1E-06	
UPR-39B	rz	129.8	1.44	0.383	2.33	1.42	0.401	2.37	1.4E-12	
UPR-39A	pcn	129.8	1.55	0.341	2.35	1.49	0.400	2.48	2.5E-06	
UPR-38	pcn	135.9	1.05	0.550	2.34	1.03	0.573	2.41	2.3E-06	

Table I-3. Yucca Wash vertical transect physical properties, dry bulk density, porosity, and particle density calculated using relative-humidity oven and 105°C oven-dry weights; saturated hydraulic conductivity and sorptivity calculated from imbibition experiments. Estimates of saturated hydraulic conductivity done using regression equations in table 3.--Continued

Sample ID	Litho-logy	Transect distance (m)	Relative-humidity oven dried			105°C oven dried			Measured saturated hydraulic conduc-tivity (m/s)	Estimated saturated hydraulic conductivity (m/s)
			Dry bulk density (g/cm^3)	Porosity (cm^3/cm^3)	Particle density (g/cm^3)	Dry bulk density (g/cm^3)	Porosity (cm^3/cm^3)	Particle density (g/cm^3)		
UPR-37	pcn	138.4	1.17	0.504	2.35	1.14	0.528	2.42	1.8E-06	
UPR-36	pcn	140.5	1.16	0.504	2.34	1.11	0.557	2.51	1.9E-06	
UPR-35	pcn	142.3	1.18	0.498	2.34	1.15	0.523	2.41	2.5E-06	
UPR-34	pcn	144.3	1.22	0.480	2.34	1.19	0.505	2.41	9.5E-07	
UPR-33	pcn	145.5	1.24	0.474	2.35	1.19	0.521	2.48	3.8E-07	
UPR-32	pcn	147.4	1.24	0.468	2.34	1.22	0.491	2.40	2.0E-07	
UPR-31	pcn	149.5	1.20	0.485	2.33	1.18	0.505	2.38	2.4E-07	
UPR-30	pcn	151.0	1.15	0.503	2.32	1.13	0.531	2.40	5.3E-07	
UPR-29	pcn	152.6	1.30	0.433	2.30	1.27	0.462	2.37	6.3E-09	
UPR-28	pcn	154.4	1.51	0.379	2.42	1.49	0.394	2.46	6.3E-09	
UPR-27	pcpw	156.1	1.53	0.389	2.50	1.52	0.398	2.53	2.1E-07	
UPR-26	pcpw	157.9	1.66	0.341	2.52	1.65	0.354	2.55	3.1E-08	
UPR-25	pcpw	160.0	1.73	0.313	2.51	1.72	0.322	2.53	3.2E-08	
UPR-24	pcpw	162.9	1.90	0.240	2.50	1.89	0.250	2.52	3.9E-09	
UPR-23	pcpw	164.3	2.03	0.196	2.52	2.01	0.210	2.55		7.3E-11
UPR-22	pcpw	165.8	1.93	0.235	2.52	1.92	0.242	2.54	1.7E-08	
UPR-21	pcpw	167.3	1.85	0.270	2.54	1.85	0.275	2.55	2.6E-08	
UPR-20	pcpw	169.5	1.88	0.256	2.53	1.86	0.272	2.56	1.9E-09	
UPR-19	pcpw	170.5	1.83	0.272	2.51	1.81	0.291	2.55	7.5E-09	
UPR-18	pcpw	172.2	1.83	0.265	2.49	1.80	0.290	2.54	8.0E-09	
UPR-17	pcpw	173.1	1.92	0.232	2.50	1.88	0.267	2.57	1.9E-09	
UPR-16	pcpw	174.0	1.90	0.240	2.49	1.86	0.272	2.56	1.2E-09	
UPR-15	pcpw	180.4	2.17	0.123	2.48	2.11	0.182	2.59	7.0E-11	
UPR-14	pcpw	185.2	1.90	0.265	2.58	1.89	0.279	2.62	2.1E-09	
UPR-13	pcpw	187.6	1.94	0.225	2.50	1.93	0.234	2.52	2.9E-10	
UPR-12	pcpw	188.7	1.97	0.201	2.47	1.93	0.237	2.54	6.0E-11	
UPR-11	pcpw	190.0	1.81	0.239	2.38	1.76	0.297	2.50	1.2E-10	
UPR-10	pcn	193.2	1.58	0.288	2.22	1.49	0.372	2.38	1.5E-10	
UPR-9	pcn	199.0	1.60	0.266	2.17	1.50	0.357	2.34	5.0E-11	
UPR-8	pcn	200.4	1.63	0.237	2.13	1.53	0.334	2.30	1.0E-10	
UPR-7	pcn	201.9	1.41	0.367	2.24	1.33	0.455	2.43	1.4E-09	
UPR-6	pcn	203.5	1.39	0.382	2.25	1.31	0.463	2.44	6.6E-10	
UPR-5	pcn	210.2	1.31	0.414	2.24	1.23	0.494	2.44		1.1E-09
UPR-4	tn	210.8	1.41	0.365	2.23	1.33	0.448	2.41	3.4E-06	
UPR-3	tn	211.7	1.66	0.359	2.59	1.64	0.376	2.64	6.9E-07	
UPR-2	tc	212.8	2.30	0.026	2.36	2.38	0.033	2.46		1.5E-10
UPR-1	tc	212.4	2.40	0.013	2.43	2.46	0.021	2.51		2.9E-10
CRT-7	tn	212.0	1.66	0.230	2.16	1.58	0.316	2.31	1.0E-07	
CRT-6	tn	212.1	1.68	0.233	2.19	1.61	0.310	2.33	2.9E-08	
CRT-5	tn	212.1	1.93	0.139	2.24	1.83	0.237	2.40	4.8E-11	
CRT-3	tc	213.1	2.41	0.007	2.43	2.40	0.021	2.45		4.4E-10

Table I-3. Yucca Wash vertical transect physical properties, dry bulk density, porosity, and particle density calculated using relative-humidity oven and 105°C oven-dry weights; saturated hydraulic conductivity and sorptivity calculated from imbibition experiments. Estimates of saturated hydraulic conductivity done using regression equations in table 3.--Continued

Sample ID	Litho-logy	Transect distance (m)	Relative-humidity oven dried			105°C oven dried			Measured saturated hydraulic conduc-tivity (m/s)	Estimated saturated hydraulic conductivity (m/s)
			Dry bulk density (g/cm³)	Porosity (cm³/cm³)	Particle density (g/cm³)	Dry bulk density (g/cm³)	Porosity (cm³/cm³)	Particle density (g/cm³)		
CRT-2	tc	213.1	2.43	0.066	2.60	2.43	0.070	2.61		2.6E-10
CRT-1	tc	216.6	2.36	0.075	2.55	2.36	0.079	2.56	5.3E-10	
LPR-32	tc	216.6	2.49	0.013	2.53	2.49	0.017	2.53	3.8E-09	
LPR-31	tc	217.0	2.39	0.069	2.57	2.39	0.074	2.58		3.2E-10
LPR-30	tr	219.5	2.30	0.082	2.50	2.29	0.086	2.51	4.0E-10	
LPR-29	tr	222.4	2.32	0.089	2.54	2.31	0.092	2.55	4.1E-09	
LPR-28	tr	224.6	2.32	0.05	2.45	2.31	0.09	2.54		9.5E-12
LPR-27	tul	227.7	2.1	0.15	2.47	2.09	0.19	2.58		3.8E-10
LPR-26	tul	231.6	2.29	0.078	2.48	2.28	0.081	2.48		2.8E-11
LPR-25	tmn	233.3	2.24	0.099	2.48	2.22	0.112	2.51	7.7E-11	
LPR-24	tmn	236.4	2.26	0.089	2.50	2.24	0.107	2.51	2.8E-12	
LPR-23	tmn	237.9	2.24	0.099	2.48	2.23	0.105	2.49	1.0E-12	
LPR-22	tmn	239.7	2.26	0.089	2.48	2.26	0.091	2.49		4.2E-11
LPR-21	tll	241.6	2.23	0.080	2.43	2.21	0.102	2.46		3.1E-11
LPR-19	tll	247.3	2.31	0.067	2.47	2.30	0.070	2.48		1.9E-11
LPR-18	tll	248.9	2.32	0.062	2.47	2.32	0.066	2.48		1.5E-11
LPR-17	tll	251.5	2.38	0.044	2.49	2.37	0.056	2.51		7.5E-12
LPR-16	tll	254.1	2.40	0.028	2.47	2.40	0.035	2.48		4.0E-12
LPR-15	tv	256.8	2.42	0.023	2.48	2.41	0.032	2.49	1.4E-10	
LPR-10	tv	267.0	2.34	0.011	2.37	2.33	0.019	2.38	3.5E-11	
LPR-7	tv	273.3	2.16	0.055	2.29	2.12	0.099	2.35	2.1E-10	
LPR-6A	Tht	276.3	1.60	0.232	2.08	1.53	0.314	2.23	7.0E-11	
LPR-6B	Tht	276.3	1.64	0.204	2.06	1.52	0.313	2.21	3.5E-10	
LPR-5	Tht	279.8	1.62	0.204	2.04	1.53	0.299	2.18		3.9E-10
LPR-4	Tht	284.4	1.53	0.320	2.25	1.45	0.397	2.41		3.0E-10
LPR-3B	Tht	286.8	1.50	0.301	2.15	1.40	0.359	2.18	1.0E-10	
LPR-3A	Tht	286.8	1.45	0.304	2.09	1.43	0.378	2.29	6.5E-11	
LPR-2	Tht	288.6	1.48	0.319	2.17	1.40	0.398	2.33	3.7E-10	
LPR-1	Tht	290.2	1.42	0.306	2.05	1.34	0.387	2.19	7.1E-11	

Table I-4. Pagany Wash vertical transect physical properties, dry bulk density, porosity, and particle density calculated using relative-humidity oven and 105°C oven-dry weights; saturated hydraulic conductivity and sorptivity calculated from imbibition experiments on relative-humidity-dried samples

Sample ID	Lithology	Transect distance (m)	Relative-humidity oven dried			105°C oven dried			Saturated hydraulic conductivity (m/s)
			Dry bulk density (g/cm^3)	Porosity (cm^3/cm^3)	Particle density (g/cm^3)	Dry bulk density (g/cm^3)	Porosity (cm^3/cm^3)	Particle density (g/cm^3)	
PW20	ccr	0.0	2.30	0.091	2.53	2.30	0.092	2.53	1.2E-09
PW19	ccr	0.0	2.29	0.095	2.54	2.29	0.097	2.54	
PW18	ccr	0.2	2.16	0.155	2.56	2.16	0.156	2.56	3.9E-09
PW17	ccr	1.5	2.27	0.108	2.55	2.27	0.109	2.55	
PW16	ccr	2.1	2.20	0.128	2.52	2.20	0.129	2.52	
PW15	ccr	3.0	2.18	0.132	2.51	2.18	0.134	2.52	
PW14	ccr	5.8	1.93	0.238	2.53	1.93	0.239	2.53	
PW13	ccr	7.6	1.92	0.243	2.53	1.91	0.246	2.54	
PW12	ccr	9.4	1.93	0.245	2.55	1.92	0.246	2.55	
PW11	ccr	11.0	1.82	0.290	2.56	1.82	0.291	2.56	
PW10	ccr	11.9	1.86	0.278	2.58	1.86	0.280	2.58	
PW9	ccr	13.4	1.89	0.267	2.57	1.88	0.269	2.58	
PW8	ccr	15.2	1.81	0.287	2.54	1.81	0.288	2.55	
PW7	ccr	16.9	1.89	0.264	2.57	1.89	0.265	2.57	
PW6	cuc	18.6	2.07	0.187	2.54	2.07	0.187	2.55	
PW5	cuc	19.5	1.97	0.227	2.55	1.97	0.228	2.55	
PW4	cuc	21.0	2.05	0.197	2.55	2.05	0.198	2.55	
PW3	cuc	22.1	2.03	0.198	2.53	2.03	0.199	2.53	
PW2	cul	23.5	2.13	0.156	2.52	2.13	0.157	2.52	
PW1	cul	25.0	2.13	0.157	2.52	2.12	0.159	2.52	

Table I-5. Calico Hills Formation vertical transect physical properties, dry bulk density, porosity, and particle density calculated using relative humidity oven and 105°C oven-dry weights; saturated hydraulic conductivity and sorptivity calculated from imbibition experiments on relative-humidity-dried samples

Sample ID	Litho-logy	Transect distance (m)	Relative-humidity oven dried: Dry bulk density (g/cm^3)	Relative-humidity oven dried: Porosity (cm^3/cm^3)	Relative-humidity oven dried: Particle density (g/cm^3)	105°C oven dried: Dry bulk density (g/cm^3)	105°C oven dried: Porosity (cm^3/cm^3)	105°C oven dried: Particle density (g/cm^3)	Saturated hydraulic conduc-tivity (m/s)	RH-dried sorptivity (m/s$^{0.5}$)
CH64	Thtz	0.0	2.11	0.104	2.35	2.09	0.126	2.39		
CH63	Thtz	1.8	1.94	0.137	2.25	1.87	0.201	2.34		
CH62	Thtz	2.7	1.99	0.083	2.17	1.89	0.178	2.30		
CH61	Thtz	4.6	1.80	0.158	2.14	1.71	0.249	2.28		
CH59G	Thtz	7.9	1.61	0.215	2.05	1.52	0.302	2.18		
CH59R*	Thtz	7.9	1.60	0.231	2.08	1.51	0.317	2.21		
CH58	Thtz	9.3	1.71	0.181	2.09	1.62	0.269	2.22		
CH57	Thtz	10.7	1.51	0.285	2.11	1.43	0.366	2.25		
CH56	Thtz	11.9	1.68	0.215	2.14	1.59	0.300	2.28		
CH55	Thtz	13.6	1.62	0.263	2.20	1.53	0.351	2.36		
CH54	Thtz	15.1	1.42	0.308	2.05	1.35	0.380	2.17		
CH53	Thtz	16.9	1.56	0.278	2.15	1.47	0.360	2.30		
CH52	Thtz	18.3	1.59	0.267	2.16	1.50	0.353	2.32		
CH51	Thtz	19.8	1.66	0.254	2.23	1.59	0.324	2.36		
CH50	Thtz	22.3	1.60	0.278	2.22	1.52	0.355	2.36		
CH49	Thtz	23.8	1.71	0.230	2.22	1.63	0.314	2.37		
CH48	Thtz	25.0	1.74	0.217	2.23	1.66	0.304	2.38		
CH47	Thtz	26.4	1.72	0.231	2.23	1.63	0.313	2.38	2.9E-11	
CH46	Thtz	27.9	1.77	0.203	2.22	1.69	0.286	2.37		
CH45	Thtz	29.6	1.74	0.216	2.22	1.65	0.300	2.36		
CH44	Thtz	30.8	1.67	0.223	2.15	1.59	0.302	2.28	8.4E-11	
CH43	Thtz	32.3	1.54	0.303	2.21	1.46	0.380	2.36		
CH42	Thtz	33.5	1.62	0.260	2.19	1.55	0.334	2.33		
CH41	Thtz	34.9	1.58	0.291	2.22	1.51	0.362	2.36		
CH40	Thtz	36.4	1.56	0.294	2.21	1.50	0.354	2.32	2.1E-10	
CH39	Thtz	37.9	1.63	0.277	2.26	1.58	0.332	2.36		
CH38	Thtz	39.3	1.61	0.280	2.23	1.54	0.341	2.34		
CH37	Thtz	40.8	1.75	0.213	2.22	1.66	0.301	2.37		
CH36	Thtz	42.4	1.77	0.213	2.25	1.69	0.294	2.39		
CH35	Thtz	43.9	1.72	0.223	2.21	1.64	0.301	2.34		
CH34	Thtz	44.8	1.73	0.218	2.22	1.65	0.298	2.36		
CH35A	Thtz	44.8	1.76	0.217	2.25	1.66	0.311	2.41		
CH33	Thtz	46.5	1.78	0.211	2.25	1.70	0.291	2.39	4.6E-12	
CH32	Thtz	48.0	1.72	0.229	2.24	1.65	0.308	2.38		1.4E-05
CH31B	Thtz	49.7	1.65	0.255	2.22	1.58	0.329	2.35		
CH31A	Thtz	49.7	1.78	0.211	2.25	1.71	0.281	2.38		
CH30	Thtz	51.2	1.84	0.206	2.32	1.80	0.251	2.40		
CH29	Thtz	52.7	1.58	0.275	2.18	1.53	0.332	2.29		
CH28	Thtz	55.5	1.39	0.371	2.22	1.34	0.425	2.33		
CH27	Thtz	57.8	1.50	0.305	2.16	1.44	0.362	2.26		
CH26	Thtz	59.1	1.54	0.281	2.13	1.48	0.339	2.23		
CH25	Thtz	60.4	1.49	0.302	2.14	1.43	0.359	2.24		3.1E-05

Table I-5. Calico Hills Formation vertical transect physical properties, dry bulk density, porosity, and particle density calculated using relative humidity oven and 105°C oven-dry weights; saturated hydraulic conductivity and sorptivity calculated from imbibition experiments on relative-humidity-dried samples--Continued

Sample ID	Litho-logy	Transect distance (m)	Relative-humidity oven dried: Dry bulk density (g/cm^3)	Relative-humidity oven dried: Porosity (cm^3/cm^3)	Relative-humidity oven dried: Particle density (g/cm^3)	105°C oven dried: Dry bulk density (g/cm^3)	105°C oven dried: Porosity (cm^3/cm^3)	105°C oven dried: Particle density (g/cm^3)	Saturated hydraulic conduc-tivity (m/s)	RH-dried sorptivity ($m/s^{0.5}$)
CH24	Thtz	61.6	1.48	0.307	2.14	1.42	0.370	2.25		
CH23	Thtz	63.1	1.42	0.327	2.10	1.35	0.392	2.22		
CH22	Thtz	64.9	1.54	0.305	2.22	1.48	0.368	2.34		
CH21	Thtz	65.8	1.43	0.317	2.10	1.38	0.374	2.20		1.4E-05
CH20	Thtz	66.8	1.42	0.356	2.20	1.36	0.413	2.31		
CH19	Thtz	68.0	1.37	0.382	2.22	1.32	0.432	2.32		
CH18	Thtz	69.6	1.43	0.314	2.09	1.37	0.375	2.19		2.1E-05
CH17	Thtz	71.0	1.52	0.301	2.17	1.46	0.362	2.28		
CH16	Thtz	72.5	1.56	0.293	2.21	1.50	0.356	2.33		
CH15	Thtz	74.2	1.50	0.304	2.15	1.44	0.365	2.26		
CH14	Thtz	75.6	1.44	0.371	2.29	1.38	0.430	2.42		
CH13	Thtz	75.7	1.57	0.293	2.22	1.51	0.357	2.34		
CH12	Thtz	77.1	1.75	0.222	2.25	1.69	0.287	2.37		
CH11	Thtz	78.6	1.54	0.312	2.23	1.48	0.371	2.35		
CH10	Thtz	80.2	1.47	0.339	2.23	1.42	0.392	2.34		
CH9	Thtz	81.4	1.50	0.323	2.21	1.44	0.381	2.33		
CH8	Thtz	83.8	1.55	0.303	2.22	1.49	0.362	2.34		
CH7	Thtz	86.0	1.61	0.304	2.31	1.55	0.363	2.44		
CH6	Thtz	87.5	1.67	0.257	2.25	1.61	0.317	2.36		
CH5	Thtz	89.0	1.62	0.296	2.30	1.57	0.347	2.41		
CH4	Thtz	93.6	1.93	0.189	2.38	1.88	0.239	2.47	1.1E-10	1.2E-05
CH3	Thtz	94.8	1.90	0.203	2.38	1.86	0.241	2.45		
CH2	pp	99.1	1.61	0.370	2.55	1.60	0.372	2.56		
CH1	pp	101.5	2.24	0.121	2.55	2.24	0.123	2.55		

* R specifies red alteration of sample, which is about 2 cm above the sample with green alteration, G.

Table I-6. Yucca Crest horizontal transect physical properties, dry bulk density, porosity, and particle density calculated using relative-humidity oven and 105°C oven-dry weights; saturated hydraulic conductivity and sorptivity calculated from imbibition experiments on relative-humidity-dried samples

Sample ID	Lithology	Transect distance (m)	Relative-humidity oven dried			105°C oven dried			Saturated hydraulic conductivity (m/s)
			Dry bulk density (g/cm³)	Porosity (cm³/cm³)	Particle density (g/cm³)	Dry bulk density (g/cm³)	Porosity (cm³/cm³)	Particle density (g/cm³)	
1Y	cuc	0.0	1.96	0.234	2.56	1.96	0.235	2.56	4.0E-08
2Y	cuc	0.0	2.21	0.115	2.49	2.20	0.123	2.51	
3Y	cuc	152.4	1.87	0.282	2.60	1.87	0.284	2.61	
4Y	cuc	152.4	1.93	0.257	2.60	1.93	0.257	2.60	
5Y	cuc	304.8	2.04	0.182	2.49	2.03	0.186	2.50	
6Y	cuc	304.8	2.02	0.191	2.50	2.02	0.193	2.51	7.7E-09
7Y	cuc	457.2	1.98	0.228	2.56	1.98	0.229	2.56	
8Y	cuc	457.2	1.95	0.237	2.56	1.95	0.238	2.56	
9Y	cuc	609.6	2.12	0.139	2.46	2.11	0.139	2.46	
10Y	cuc	609.6	2.11	0.157	2.50	2.11	0.157	2.50	
11Y	cuc	762.0	1.91	0.256	2.56	1.90	0.257	2.56	1.4E-07
12Y	cuc	914.4	1.94	0.241	2.56	1.94	0.241	2.56	
13Y	cuc	914.4	1.93	0.247	2.56	1.93	0.247	2.56	
14Y	cuc	1,066.8	2.24	0.102	2.49	2.23	0.105	2.50	
15Y	cuc	1,219.2	1.86	0.273	2.55	1.86	0.273	2.55	
16Y	cuc	1,219.2	1.84	0.281	2.56	1.84	0.283	2.57	
17Y	cuc	1,371.6	1.94	0.240	2.56	1.94	0.241	2.56	
18Y	cuc	1,371.6	1.90	0.233	2.48	1.90	0.234	2.48	
19Y	cuc	1,524.0	2.02	0.208	2.55	2.02	0.208	2.55	
20Y	cuc	1,676.4	1.89	0.262	2.57	1.89	0.263	2.57	
21Y	cuc	1,828.8	2.02	0.212	2.57	2.02	0.212	2.57	
22Y	cuc	1,981.2	2.08	0.192	2.57	2.07	0.195	2.57	
23Y	cuc	2,133.6	1.89	0.243	2.50	1.89	0.243	2.50	
24Y	cuc	2,286.0	1.90	0.260	2.57	1.90	0.260	2.57	
25Y	cuc	2,438.4	1.79	0.310	2.60	1.79	0.311	2.60	
26Y	cuc	2,590.8	1.74	0.317	2.55	1.74	0.319	2.55	
27Y	cuc	2,743.2	1.94	0.246	2.58	1.94	0.247	2.58	1.0E-07
28Y	cuc	2,895.6	1.84	0.278	2.55	1.84	0.279	2.55	
29Y	cuc	3,048.0	1.99	0.222	2.56	1.99	0.222	2.56	
30Y	cuc	3,200.4	1.89	0.264	2.56	1.89	0.265	2.57	1.4E-07
31Y	cuc	3,352.8	1.94	0.248	2.58	1.94	0.249	2.58	
32Y	cuc	3,505.2	1.94	0.250	2.59	1.94	0.250	2.59	
33Y	cuc	3,657.6	1.90	0.263	2.57	1.90	0.264	2.58	
34Y	cuc	3,810.0	1.98	0.196	2.47	1.98	0.198	2.47	8.0E-09
35Y	cuc	3,962.4	1.82	0.301	2.60	1.81	0.303	2.60	
36Y	cuc	4,114.8	1.87	0.281	2.60	1.87	0.282	2.61	
37Y	cuc	4,267.2	1.83	0.280	2.54	1.83	0.280	2.55	
38Y	cuc	4,419.6	1.95	0.222	2.51	1.95	0.223	2.51	3.7E-08
39Y	cuc	4,572.0	1.93	0.249	2.57	1.93	0.252	2.58	
40Y	cuc	4,572.0	1.80	0.306	2.60	1.80	0.307	2.60	
41Y	cuc	4,724.4	2.02	0.197	2.52	2.02	0.198	2.52	
42Y	cuc	4,724.4	1.92	0.244	2.54	1.91	0.250	2.55	
43Y	cuc	4,876.8	1.89	0.264	2.56	1.88	0.264	2.56	9.8E-08
44Y	cuc	4,876.8	1.87	0.265	2.54	1.87	0.265	2.54	
45Y	cuc	5,029.2	1.95	0.241	2.57	1.95	0.242	2.58	

Table I-7. Shardy base horizontal transect physical properties, dry bulk density, porosity, and particle density calculated using relative-humidity oven-dry weights and saturated hydraulic conductivity

Sample ID	Lithology	Transect distance (m)	Relative-humidity oven dried			Saturated hydraulic conductivity (m/s)
			Dry bulk density (g/cm^3)	Porosity (cm^3/cm^3)	Particle density (g/cm^3)	
0 + 00	ccb	0.0	1.42	0.391	2.33	1.8E-06
1 + 00	ccb	30.5	1.57	0.334	2.35	7.3E-08
1 + 43	ccb	43.6	1.37	0.412	2.34	5.3E-06
2 + 05	ccb	62.5	1.32	0.430	2.32	9.3E-06
2 + 45	ccb	74.7	1.39	0.410	2.35	3.1E-06
2 + 90	ccb	88.4	1.26	0.452	2.29	9.0E-06
3 + 45	ccb	105.2	1.36	0.411	2.30	5.3E-06
3 + 65	ccb	111.3	1.47	0.374	2.35	2.8E-06
3 + 70	ccb	112.8	1.33	0.428	2.32	6.9E-06
3 + 90	ccb	118.9	1.51	0.354	2.33	1.2E-06
4 + 20	ccb	128.0	1.38	0.408	2.32	9.6E-06
4 + 60	ccb	140.2	1.40	0.397	2.33	3.4E-06
5 + 00	ccb	152.4	1.33	0.431	2.34	6.7E-06
5 + 75	ccb	175.3	1.35	0.418	2.33	8.3E-06
5 + 90	ccb	179.8	1.33	0.432	2.34	2.7E-06
6 + 10	ccb	185.9	1.39	0.406	2.34	7.1E-06
6 + 45	ccb	196.6	1.39	0.404	2.33	2.5E-06
6 + 70	ccb	204.2	1.53	0.355	2.37	8.4E-07
7 + 20	ccb	219.5	1.27	0.451	2.31	7.2E-06
7 + 50	ccb	228.6	1.41	0.400	2.35	3.0E-06
8 + 40	ccb	256.0	1.38	0.409	2.34	4.5E-06
8 + 60	ccb	262.1	1.32	0.438	2.35	8.8E-06
8 + 85	ccb	269.7	1.35	0.429	2.36	2.3E-06
8 + 90	ccb	271.3	1.41	0.409	2.38	1.5E-06
9 + 00	ccb	274.3	1.27	0.461	2.36	5.4E-06
9 + 80	ccb	298.7	1.31	0.427	2.28	5.0E-06
10 + 00	ccb	304.8	1.31	0.435	2.33	8.7E-06
10 + 20	ccb	310.9	1.30	0.443	2.34	8.7E-06
10 + 40	ccb	317.0	1.53	0.355	2.37	1.4E-07
10 + 65	ccb	324.6	1.29	0.449	2.34	3.9E-06
11 + 05	ccb	336.8	1.29	0.449	2.34	4.9E-06
11 + 25	ccb	342.9	1.29	0.454	2.35	5.2E-06
11 + 45	ccb	349.0	1.27	0.459	2.35	2.5E-06
11 + 65	ccb	355.1	1.35	0.423	2.34	2.3E-06
11 + 90	ccb	362.7	1.47	0.373	2.34	3.7E-07
12 + 20	ccb	371.9	1.62	0.313	2.37	
12 + 35	ccb	376.4	1.76	0.261	2.37	2.2E-10
12 + 80	ccb	390.1	1.53	0.353	2.37	4.1E-07
13 + 00	ccb	396.2	1.34	0.429	2.35	3.6E-06
13 + 20	ccb	402.3	1.30	0.446	2.34	2.1E-06
13 + 70	ccb	417.6	1.34	0.432	2.37	3.2E-06
13 + 90	ccb	423.7	1.29	0.451	2.34	4.7E-06
14 + 10	ccb	429.8	1.37	0.417	2.35	4.6E-07

Table I-7. Shardy base horizontal transect physical properties, dry bulk density, porosity, and particle density calculated using relative-humidity oven-dry weights and saturated hydraulic conductivity--Continued

Sample ID	Lithology	Transect distance (m)	Relative-humidity oven dried			Saturated hydraulic conductivity (m/s)
			Dry bulk density (g/cm^3)	Porosity (cm^3/cm^3)	Particle density (g/cm^3)	
14 + 30	ccb	435.9	1.34	0.429	2.34	9.4E-07
14 + 50	ccb	442.0	1.44	0.377	2.31	7.3E-07
14 + 70	ccb	448.1	1.40	0.400	2.33	4.5E-06
14 + 95	ccb	455.7	1.32	0.432	2.33	7.3E-06
15 + 15	ccb	461.8	1.42	0.388	2.32	5.2E-06
15 + 40	ccb	469.4	1.86	0.222	2.39	4.8E-11
15 + 70	ccb	478.5	1.70	0.283	2.37	1.6E-08
16 + 20	ccb	493.8	1.58	0.334	2.37	1.1E-07
16 + 40	ccb	499.9	1.53	0.352	2.36	5.2E-07
16 + 65	ccb	507.5	1.53	0.348	2.35	1.2E-07
16 + 85	ccb	513.6	1.35	0.426	2.36	2.7E-06
17 + 05	ccb	519.7	1.43	0.393	2.35	4.5E-06
17 + 25	ccb	525.8	1.35	0.430	2.36	3.3E-06
20 + 85	ccb	635.5	1.35	0.411	2.28	5.3E-06
21 + 05	ccb	641.6	1.40	0.393	2.30	5.9E-06
21 + 40	ccb	652.3	1.44	0.391	2.36	3.1E-07
21 + 75	ccb	662.9	1.32	0.434	2.34	5.4E-06
21 + 95	ccb	669.0	1.32	0.434	2.33	8.7E-06
22 + 15	ccb	675.1	1.37	0.397	2.28	2.9E-06
22 + 60	ccb	688.8	1.35	0.414	2.31	8.4E-06
22 + 80	ccb	694.9	1.35	0.413	2.30	1.0E-05
23 + 00	ccb	701.0	1.32	0.421	2.28	6.5E-06

Table I-8. Topopah Spring Tuff vitric caprock horizontal transect physical properties, dry bulk density, porosity, and particle density calculated using relative-humidity oven and 105°C oven-dry weights; saturated hydraulic conductivity and sorptivity calculated using imbibition experiments on relative-humidity-dried samples. Transect distance is zero at borehole USW-UZ6s, and positive is north.

Sample ID	Litho-logy	Transect distance (m)	Relative-humidity oven dried			105°C oven dried			Saturated hydraulic conductivity (m/s)
			Dry bulk density (g/cm³)	Porosity (cm³/cm³)	Particle density (g/cm³)	Dry bulk density (g/cm³)	Porosity (cm³/cm³)	Particle density (g/cm³)	
TC46	tc	-247.5	2.37	0.017	2.41	2.37	0.019	2.41	
TC45	tc	-228.6	2.37	0.011	2.39	2.36	0.014	2.40	
TC44	tc	-198.1	2.37	0.016	2.40	2.36	0.018	2.41	2.7E-09
TC43	tc	-173.7	2.37	0.015	2.41	2.37	0.017	2.41	2.0E-09
TC42	tc	-132.3	2.36	0.019	2.40	2.35	0.022	2.41	2.8E-09
TC41	tc	-98.5	2.50	0.011	2.52	2.49	0.016	2.53	
TC40	tc	-63.4	2.41	0.026	2.47	2.41	0.028	2.47	7.4E-09
TC39	tc	-42.7	2.36	0.024	2.42	2.36	0.026	2.42	1.4E-09
TC38	tc	-30.5	2.36	0.076	2.55	2.35	0.077	2.55	2.1E-09
TC1	tc	36.6	2.32	0.043	2.42	2.32	0.045	2.43	
TC2	tc	67.1	2.39	0.028	2.46	2.39	0.031	2.46	
TC3	tc	85.3	2.49	0.015	2.53	2.48	0.021	2.53	
TC4	tc	144.8	2.43	0.011	2.45	2.42	0.013	2.46	
TC5	tc	189.6	2.41	0.017	2.45	2.41	0.020	2.45	
TC6	tc	210.3	2.42	0.010	2.45	2.42	0.013	2.45	
TC7	tc	248.7	2.41	0.015	2.45	2.41	0.018	2.45	1.7E-08
TC8	tc	271.9	2.46	0.036	2.55	2.46	0.038	2.56	
TC9	tc	294.7	2.37	0.015	2.41	2.37	0.017	2.41	3.0E-09
TC10	tc	320.0	2.37	0.017	2.41	2.37	0.019	2.41	
TC11B	tc	365.8	2.41	0.023	2.46	2.41	0.024	2.47	1.6E-09
TC11R	tc	365.8	2.40	0.029	2.47	2.40	0.031	2.48	8.3E-09
TC12	tc	403.3	2.43	0.013	2.46	2.43	0.014	2.46	
TC13	tc	414.5	2.40	0.017	2.44	2.40	0.018	2.44	1.8E-07
TC13A	tc	414.6	2.45	0.017	2.49	2.44	0.021	2.50	
TC14	tc	466.3	2.41	0.020	2.46	2.41	0.022	2.46	9.5E-10
TC15	tc	490.7	2.37	0.020	2.42	2.37	0.022	2.42	5.6E-09
TC16	tc	559.3	2.26	0.102	2.51	2.25	0.104	2.52	
TC17	tc	632.5	2.41	0.047	2.53	2.41	0.050	2.54	
TC18	tc	685.8	2.41	0.015	2.44	2.40	0.017	2.45	
TC19	tc	748.0	2.38	0.031	2.45	2.37	0.033	2.45	
TC20	tc	778.2	2.42	0.012	2.45	2.42	0.013	2.45	
TC21	tc	800.1	2.40	0.011	2.42	2.39	0.014	2.43	9.8E-10
TC22	tc	833.0	2.39	0.017	2.44	2.39	0.020	2.44	
TC22A	tc	833.0	2.46	0.024	2.52	2.45	0.030	2.53	
TC23	tc	891.5	2.32	0.028	2.39	2.32	0.031	2.39	1.7E-10
TC24	tc	952.5	2.41	0.013	2.45	2.41	0.016	2.45	
TC25	tc	986.0	2.41	0.015	2.45	2.41	0.016	2.45	
TC26	tc	1,011.9	2.39	0.027	2.46	2.39	0.030	2.46	
TC27	tc	1,097.3	2.31	0.055	2.45	2.31	0.059	2.45	
TC28	tc	1,145.4	2.51	0.017	2.55	2.50	0.022	2.56	
TC29	tc	1,192.4	2.38	0.056	2.52	2.37	0.058	2.52	1.7E-09

Table I-8. Topopah Spring Tuff vitric caprock horizontal transect physical properties, dry bulk density, porosity, and particle density calculated using relative-humidity oven and 105°C oven-dry weights; saturated hydraulic conductivity and sorptivity calculated using imbibition experiments on relative-humidity-dried samples. Transect distance is zero at borehole USW-UZ6s, and positive is north.--Continued

Sample ID	Litho-logy	Transect distance (m)	Relative-humidity oven dried			105°C oven dried			Saturated hydraulic conductivity (m/s)
			Dry bulk density (g/cm^3)	Porosity (cm^3/cm^3)	Particle density (g/cm^3)	Dry bulk density (g/cm^3)	Porosity (cm^3/cm^3)	Particle density (g/cm^3)	
TC30	tc	1,255.8	2.40	0.059	2.55	2.40	0.061	2.55	
TC31	tc	1,345.7	2.42	0.021	2.47	2.42	0.023	2.47	7.0E-10
TC32	tc	1,365.5	2.51	0.011	2.54	2.51	0.016	2.55	
TC33	tc	1,443.2	2.50	0.026	2.56	2.49	0.028	2.57	
TC34	tc	1,446.9	2.36	0.023	2.41	2.35	0.026	2.42	
TC35	tc	1,492.0	2.37	0.030	2.45	2.37	0.032	2.45	2.7E-09
TC36	tc	1,524.0	2.39	0.015	2.42	2.38	0.018	2.43	
TC37B	tc	1,575.8	2.43	0.021	2.48	2.43	0.025	2.49	2.7E-09
TC37R	tc	1,575.8	2.40	0.014	2.43	2.40	0.016	2.44	

APPENDIX II: MOISTURE-RETENTION MEASUREMENTS FOR SUBSAMPLES OF 41 OUTCROP TRANSECT CORES

Appendix II. Moisture-retention measurements for subsamples of 41 outcrop transect core. Data are listed as volumetric water content (VWC) versus the absolute value of water potential (BARS)

PW19s		TPC52s		TPC35s		TPC27s		TPC15s	
VWC	BARS	VWC	BARS	VWC	BARS	VWC	BARS	VWC	BARS
0.105	0.1	0.108	0.1	0.081	0.1	0.115	0.1	0.08	0.1
0.094	1.4	0.095	2.7	0.071	2.8	0.105	2.8	0.07	2.8
0.076	2.8	0.089	2.8	0.063	4.1	0.071	8.3	0.07	4.8
0.056	4.2	0.071	5.5	0.058	9.8	0.089	8.4	0.06	9.8
0.051	5.6	0.078	7.0	0.050	12.5	0.058	12.4	0.05	21.0
0.069	5.6	0.060	8.3	0.046	19.6	0.065	16.8	0.05	29.4
0.044	6.9	0.067	8.3	0.040	34.8	0.040	27.7	0.04	43.3
0.038	20.7	0.053	15.1	0.035	59.0	0.033	44.7	0.04	69.0
0.031	56.1	0.046	29.2	0.031	95.3	0.022	110.3	0.03	138.7
0.029	102.8	0.040	43.3	0.027	134.4	0.015	290.2	0.03	201.2
0.018	428.1	0.035	64.8	0.022	249.9	0.008	680.8	0.02	264.9
0.014	489.1	0.025	194.8	0.016	437.2	0.006	838.2	0.01	569.8
0.007	1,124.6	0.019	369.2	0.012	656.5	0.005	1,302.0	0.01	733.9
0.005	1,439.6	0.006	1,342.7	0.006	1,315.3	0.005	1,522.7	0.01	1,114.0
0.004	1,648.4	0.004	1,648.4	0.005	1,635.9	0.007			1,300.0

TPC9s		TPC5s		TPC2s		TPC1s		BT27Hs	
VWC	BARS	VWC	BARS	VWC	BARS	VWC	BARS	VWC	BARS
0.032	0.1	0.035	0.1	0.042	0.1	0.120	0.1	0.21	0.1
0.029	20.8	0.030	101.0	0.038	9.7	0.110	4.1	0.20	4.2
0.022	90.0	0.027	201.0	0.035	54.8	0.102	12.5	0.19	4.1
0.018	372.0	0.024	568.0	0.031	240.0	0.095	22.5	0.18	4.2
0.008	1,319.0	0.023	627.1	0.029	310.0	0.089	49.3	0.16	7.0
0.008	1,042.0	0.020	1,098.0	0.026	373.0	0.085	66.8	0.14	26.3
0.006	1,572.0	0.019	1,058.3	0.021	466.0	0.078	73.0	0.13	48.0
		0.015	2,158.1			0.074	76.3	0.10	203.2
						0.066	105.7	0.09	255.1
						0.063	137.4	0.04	2,592.1
						0.057	199.6		
						0.044	477.7		
						0.037	617.2		
						0.028	1,010.2		
						0.026	1,218.3		

BT26Hs		BT25Hs		BT24Hs		BT23-1Hs		BT22Hs	
VWC	BARS	VWC	BARS	VWC	BARS	VWC	BARS	VWC	BARS
0.235	0.1	0.346	0.1	0.406	0.1	0.411	0.1	0.43	0.1
0.224	1.4	0.321	1.4	0.388	1.4	0.392	1.4	0.40	1.4
0.215	2.8	0.229	1.4	0.364	1.4	0.326	4.2	0.33	1.4
0.175	4.2	0.219	2.8	0.331	2.8	0.237	1.4	0.28	1.4
0.175	8.4	0.193	4.2	0.268	1.4	0.176	1.4	0.20	2.8
0.114	26.2	0.184	2.8	0.186	4.2	0.126	4.2	0.15	5.6
0.082	130.3	0.175	8.4	0.127	4.2	0.104	4.2	0.13	8.3
0.038	990.6	0.097	35.2	0.105	8.4	0.093	9.8	0.06	124.7
		0.024	2,953.2	0.056	46.6	0.055	48.0	0.04	917.0
				0.015	2,943.7	0.019	2,727.2		

Appendix II. Moisture-retention measurements for subsamples of 41 outcrop transect core. Data are listed as volumetric water content (VWC) versus the absolute value of water potential (BARS)--Continued

BT18Hs		BT17s		BT11s		BT3Vs		BT2s	
VWC	BARS	VWC	BARS	VWC	BARS	VWC	BARS	VWC	BARS
0.442	0.1	0.442	0.1	0.628	0.1	0.381	0.1	0.06	0.1
0.420	1.4	0.414	2.8	0.572	1.4	0.327	1.4	0.05	1.4
0.370	1.4	0.372	2.8	0.516	1.4	0.259	1.4	0.04	1.4
0.361	1.4	0.347	2.8	0.463	4.2	0.158	1.4	0.04	5.6
0.288	2.8	0.183	2.8	0.322	4.2	0.101	2.8	0.03	12.5
0.174	4.2	0.150	7.0	0.194	5.6	0.096	5.6	0.02	384.0
0.151	5.6	0.134	12.6	0.073	43.7	0.064	7.0	0.02	428.0
0.136	8.4	0.090	69.8	0.012	2,281.5	0.021	123.2	0.01	489.0
0.076	43.7	0.022	2,723.8			0.006	1,071.2	0.01	376.1
0.022	2,863.4							0.01	877.3
								0.01	1,261.8

BT1s		TS58s		TS56s		TS54s		TS50s	
VWC	BARS	VWC	BARS	VWC	BARS	VWC	BARS	VWC	BARS
0.045	0.1	0.124	0.1	0.184	0.1	0.120	0.1	0.18	0.1
0.037	1.4	0.109	1.4	0.156	2.8	0.104	2.8	0.14	2.8
0.024	8.3	0.089	2.8	0.141	1.4	0.083	2.8	0.13	2.8
0.023	22.4	0.084	2.8	0.132	2.8	0.076	5.5	0.11	2.8
0.017	450.0	0.057	4.2	0.121	1.4	0.071	2.8	0.09	4.2
0.010	747.0	0.046	12.5	0.112	1.4	0.052	11.1	0.04	12.6
		0.038	38.0	0.086	5.6	0.046	5.6	0.02	171.4
		0.022	343.5	0.078	4.2	0.041	15.4	0.00	1,052.0
		0.015	553.8	0.069	8.4	0.034	68.3	0.03	313.7
				0.051	21.0	0.018	340.9	0.01	2,360.1
				0.024	138.4	0.010	488.9		

TS47s		TS40s		TS32s		TS29s		TS26s	
VWC	BARS	VWC	BARS	VWC	BARS	VWC	BARS	VWC	BARS
0.185	0.1	0.156	0.1	0.115	0.1	0.140	0.1	0.13	0.1
0.158	4.1	0.139	1.4	0.092	5.5	0.124	4.1	0.12	1.4
0.132	4.2	0.131	1.4	0.085	6.8	0.112	4.1	0.10	4.2
0.125	5.5	0.120	4.2	0.076	8.4	0.106	4.2	0.09	2.8
0.107	4.8	0.110	4.1	0.067	22.2	0.079	8.4	0.08	4.2
0.074	5.6	0.092	4.1	0.051	55.2	0.074	5.6	0.06	4.2
0.067	7.0	0.070	8.3	0.044	90.2	0.069	5.6	0.05	9.8
0.040	21.7	0.070	8.4	0.028	363.8	0.063	8.3	0.04	48.0
0.022	98.8	0.042	29.5	0.007	2,305.2	0.045	30.9	0.02	265.1
0.006	1,697.8	0.013	410.8			0.027	131.8	0.01	682.4
		0.007	1,709.0			0.010	1,013.7		

Appendix II. Moisture-retention measurements for subsamples of 41 outcrop transect core. Data are listed as volumetric water content (VWC) versus the absolute value of water potential (BARS)--Continued

BB68s		BB64s		BB45s		BB31s		BB16s	
VWC	BARS	VWC	BARS	VWC	BARS	VWC	BARS	VWC	BARS
0.078	0.1	0.192	0.1	0.141	0.1	0.099	0.1	0.07	0.1
0.072	4.1	0.184	1.4	0.132	4.1	0.076	4.1	0.06	5.5
0.057	29.2	0.174	4.2	0.112	4.1	0.067	5.5	0.05	12.4
0.052	40.6	0.172	4.1	0.105	5.5	0.061	5.5	0.05	13.9
0.046	50.9	0.168	1.4	0.095	4.2	0.051	7.0	0.03	75.3
0.038	77.6	0.166	4.2	0.087	18.0	0.043	12.4	0.03	113.0
0.031	175.3	0.136	2.8	0.064	48.0	0.032	52.3	0.03	180.0
0.020	541.2	0.106	7.0	0.052	84.6	0.018	595.7	0.02	350.0
0.000		0.070	20.9	0.031	313.7	0.004	2,306.3	0.02	388.6
		0.039	104.5	0.013	2,360.1			0.01	2,096.0
		0.005	2,524.9						

BB13As		BB5s		CH60s		CH47s		CH44s	
VWC	BARS	VWC	BARS	VWC	BARS	VWC	BARS	VWC	BARS
0.079	0.1	0.022	0.1	0.357	0.1	0.322	0.1	0.34	0.1
0.071	5.6	0.021	13.8	0.319	1.4	0.300	1.4	0.32	1.4
0.056	8.3	0.018	361.0	0.273	1.4	0.286	2.8	0.29	1.4
0.050	9.6	0.014	477.0	0.224	1.4	0.266	5.6	0.26	2.8
0.034	16.6	0.012	677.0	0.219	4.2	0.260	4.2	0.26	1.4
0.018	126.2	0.009	1,263.0	0.181	11.2	0.236	24.9	0.22	7.0
0.016	260.2	0.008	1,582.0	0.176	18.2	0.188	91.9	0.16	102.3
0.011	728.1	0.006	1,861.1	0.151	39.4	0.119	873.4	0.11	890.8
0.008	1,591.2			0.071	2,966.0			0.02	388.6
				0.013	2,360.1			0.01	2,096.0

CH40s	
VWC	BARS
0.401	0.1
0.370	1.4
0.324	2.8
0.312	2.8
0.266	4.2
0.277	4.2
0.269	7.0
0.238	11.1
0.156	94.8
0.106	883.4

APPENDIX III: GRAPHS OF MOISTURE-RETENTION DATA AND CURVE FITS FOR SUBSAMPLES OF 41 OUTCROP TRANSECT CORES

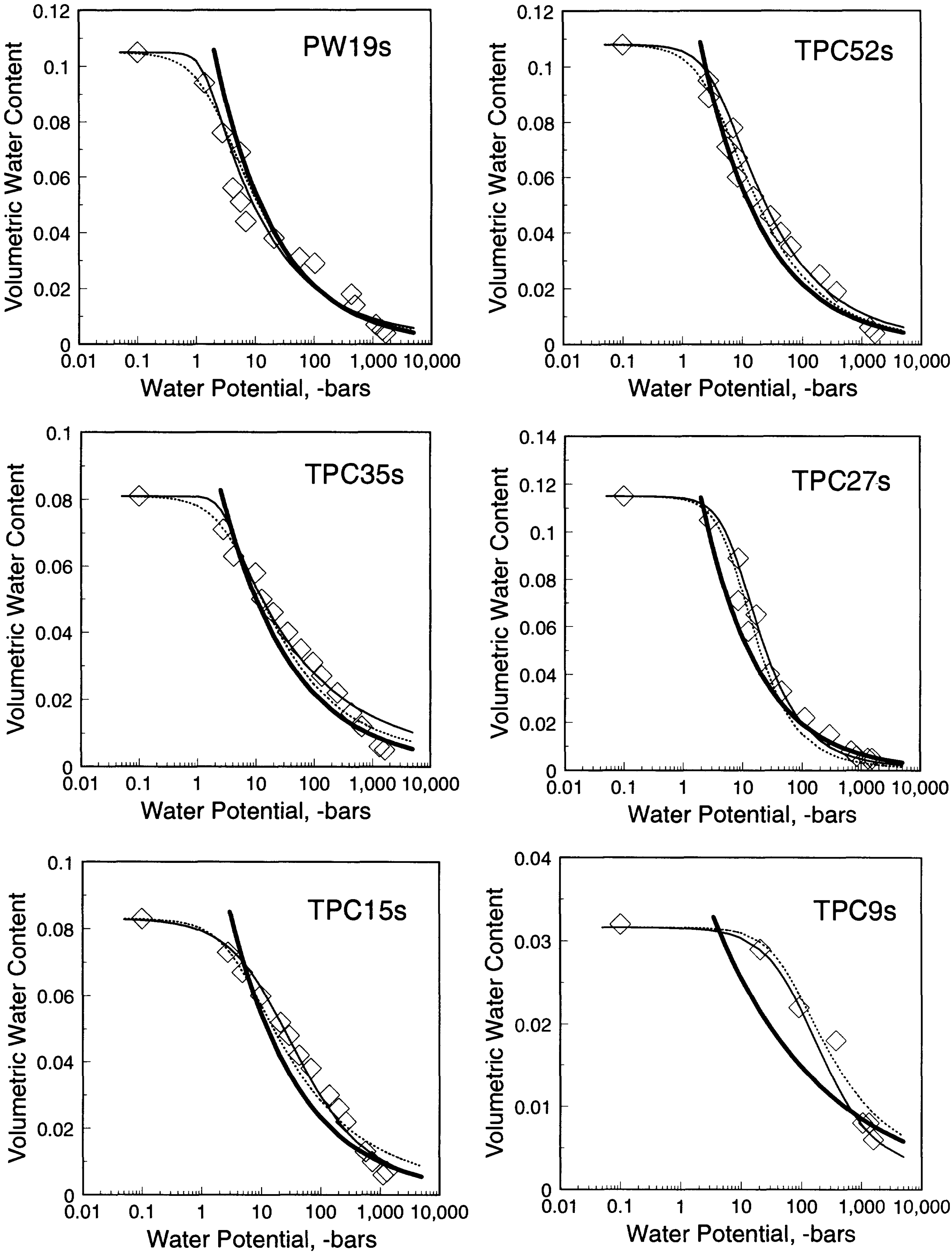

Appendix III. Points are measured data; explanation for models: narrow solid line is van Genuchten using a calculated *m* value, dotted line is van Genuchten using an estimated *m* value, and thick solid line is Brooks and Corey.

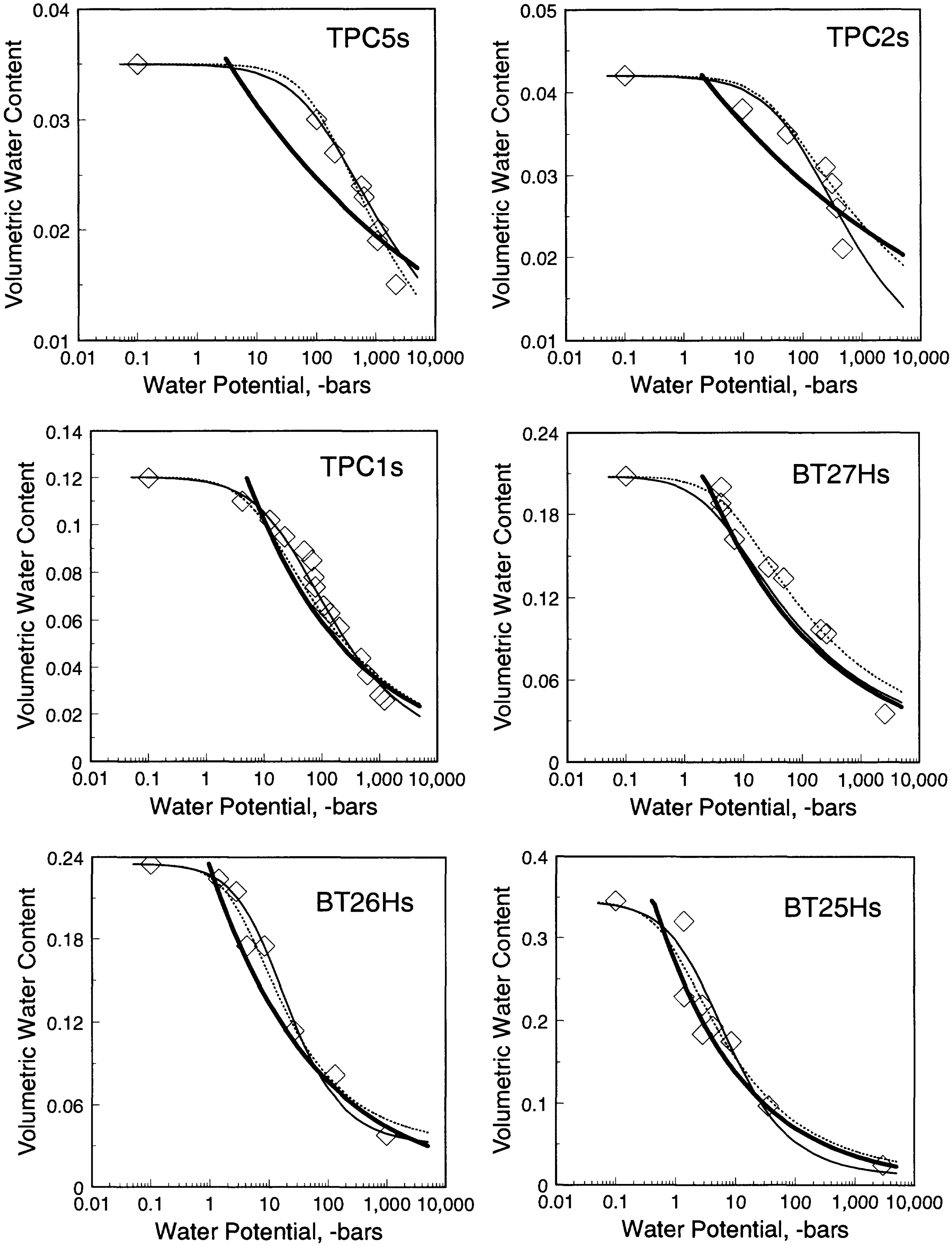

Appendix III. Points are measured data; explanation for models: narrow solid line is van Genuchten using a calculated *m* value, dotted line is van Genuchten using an estimated *m* value, and thick solid line is Brooks and Corey.--Continued

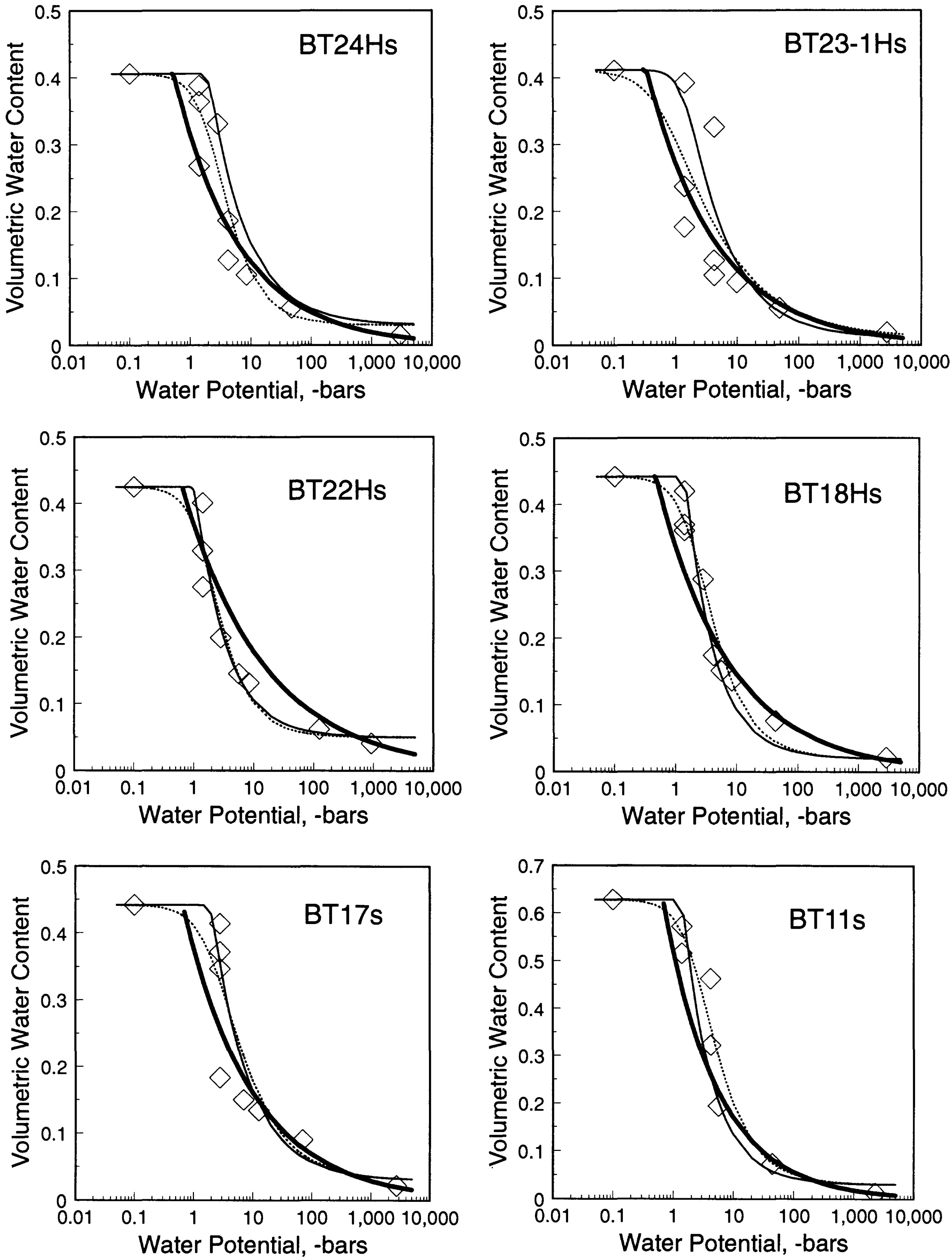

Appendix III. Points are measured data; explanation for models: narrow solid line is van Genuchten using a calculated *m* value, dotted line is van Genuchten using an estimated *m* value, and thick solid line is Brooks and Corey.--Continued

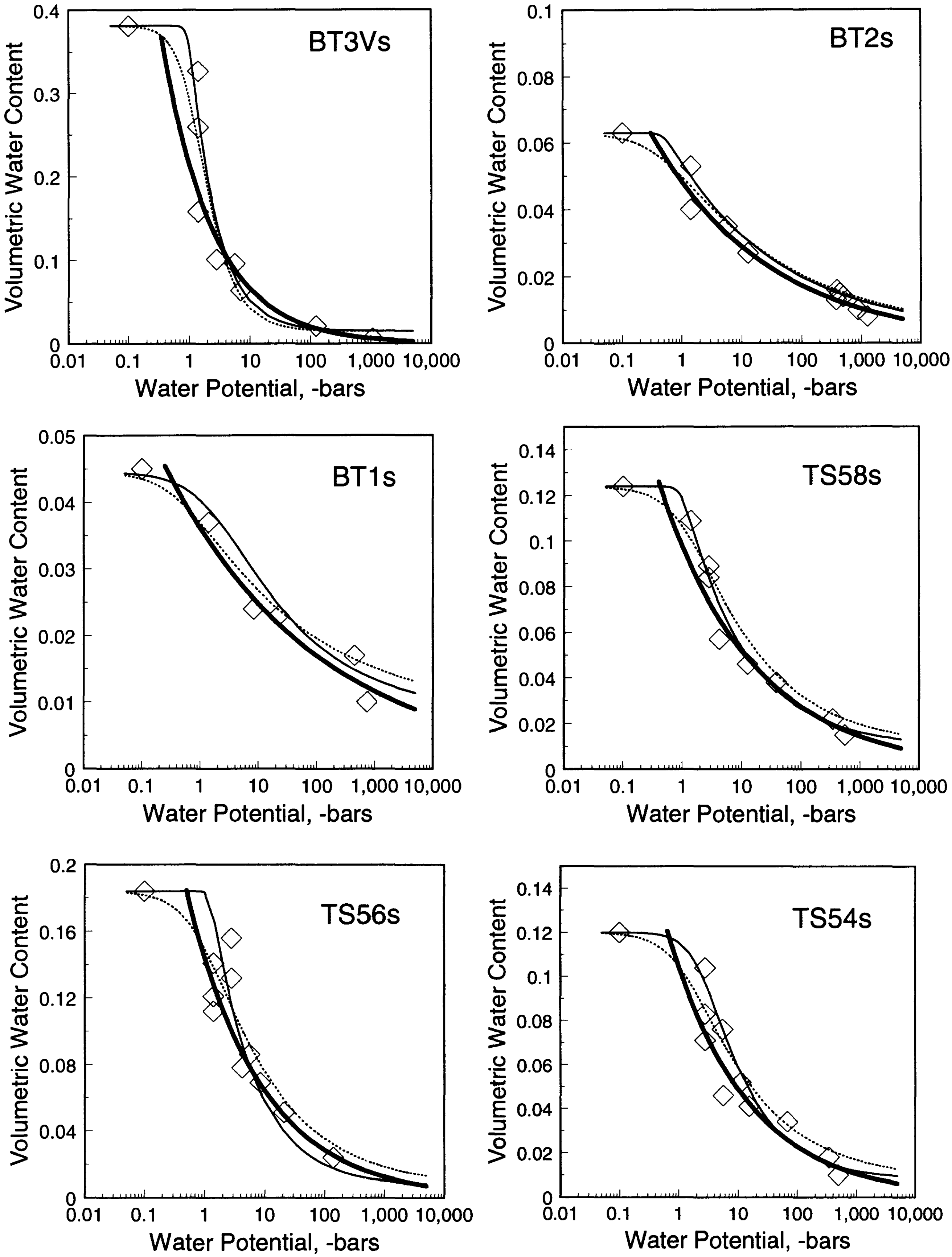

Appendix III. Points are measured data; explanation for models: narrow solid line is van Genuchten using a calculated *m* value, dotted line is van Genuchten using an estimated *m* value, and thick solid line is Brooks and Corey.--Continued

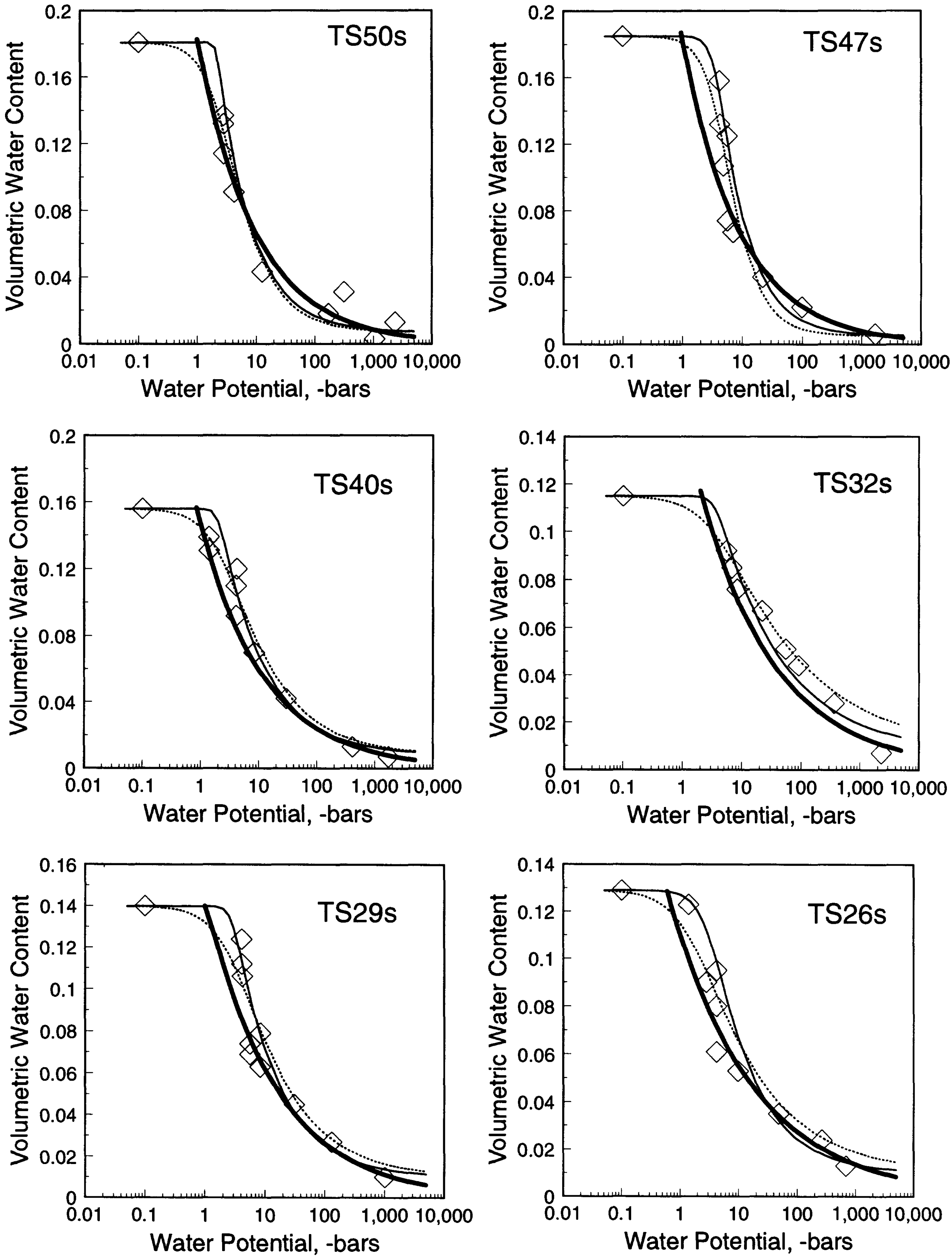

Appendix III. Points are measured data; explanation for models: narrow solid line is van Genuchten using a calculated *m* value, dotted line is van Genuchten using an estimated *m* value, and thick solid line is Brooks and Corey.--Continued

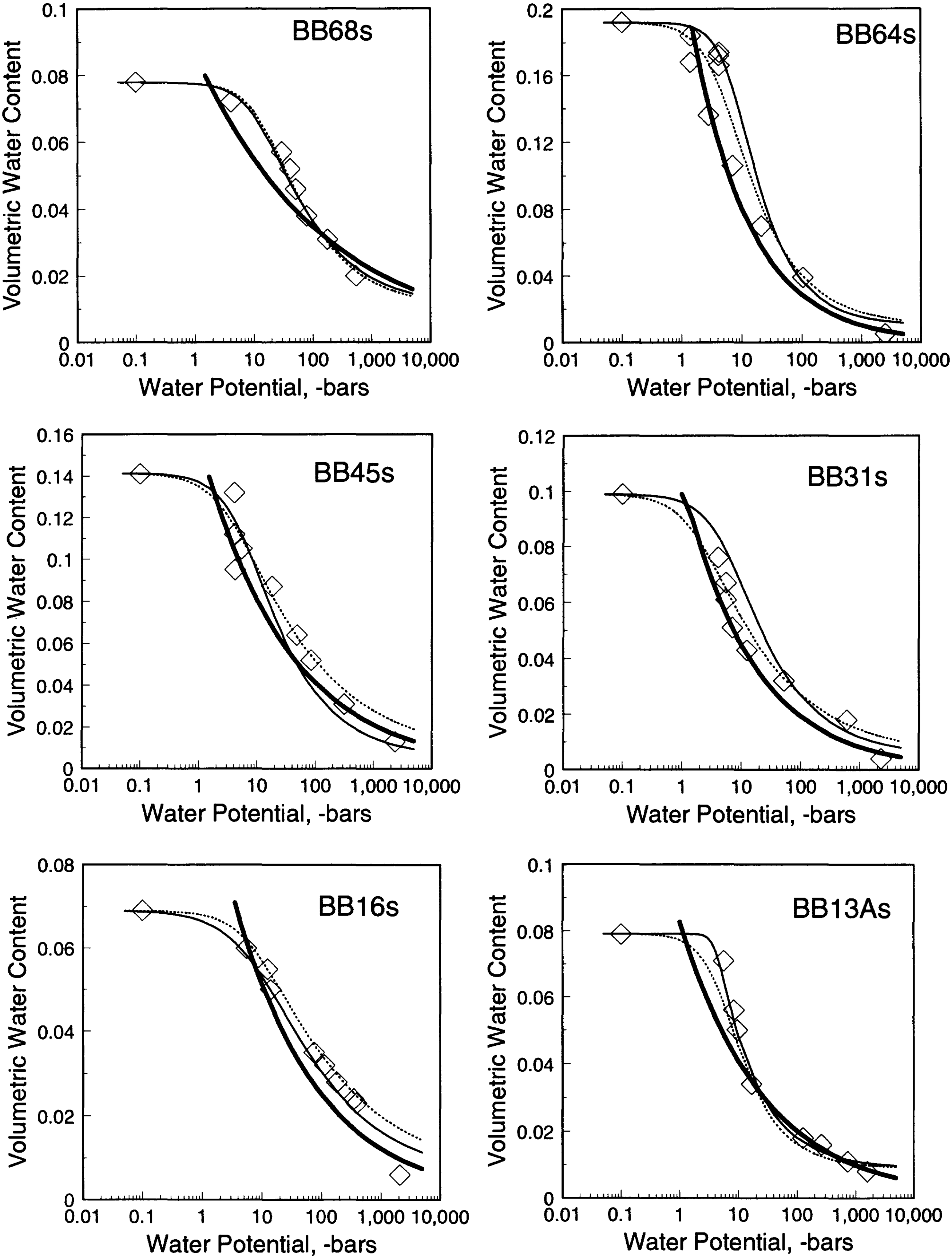

Appendix III. Points are measured data; explanation for models: narrow solid line is van Genuchten using a calculated *m* value, dotted line is van Genuchten using an estimated *m* value, and thick solid line is Brooks and Corey.--Continued

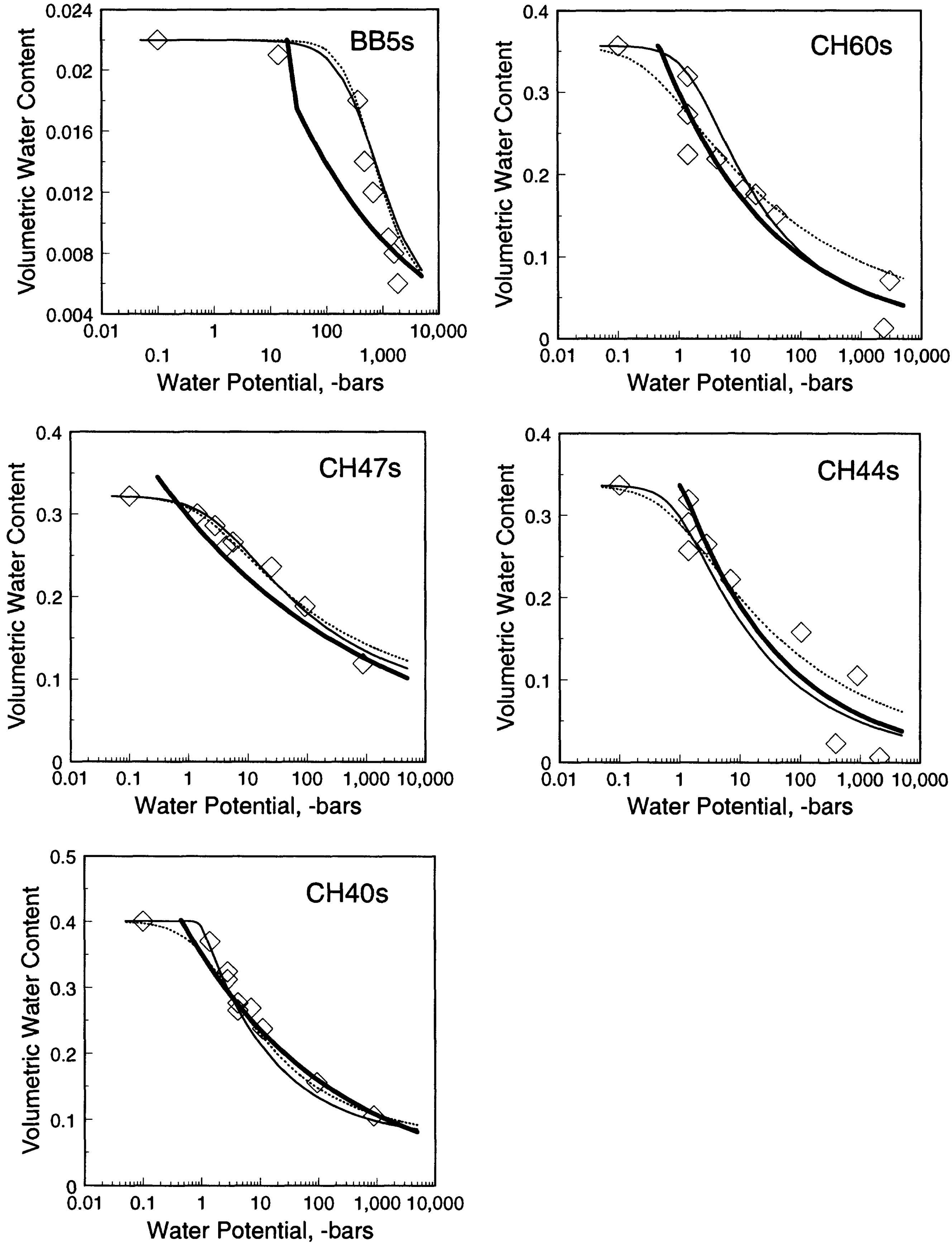

Appendix III. Points are measured data; explanation for models: narrow solid line is van Genuchten using a calculated *m* value, dotted line is van Genuchten using an estimated *m* value, and thick solid line is Brooks and Corey.--Continued

☆ U.S. GOVERNMENT PRINTING OFFICE: 1996 - 774-216 / 00111 REGION NO. 8